Naval Research Laboratory
Washington, DC 20375-5320

NRL/6120/MR—2022/1

Inorganic Cyanophosphine Rubbers

BRIAN CHALOUX

Materials Synthesis and Processing Section
Chemistry Division

February 8, 2022

REPORT DOCUMENTATION PAGE

Form Approved
OMB No. 0704-0188

1. REPORT DATE *(DD-MM-YYYY)*	**2. REPORT TYPE**	**3. DATES COVERED** *(From - To)*
08-02-2022	NRL Memorandum Report	09-05-2017 – 09-04-2018

4. TITLE AND SUBTITLE

Inorganic Cyanophosphine Rubbers

5a. CONTRACT NUMBER

5b. GRANT NUMBER

5c. PROGRAM ELEMENT NUMBER
NISE

6. AUTHOR(S)

Brian L. Chaloux

5d. PROJECT NUMBER

5e. TASK NUMBER

5f. WORK UNIT NUMBER
N2M7

7. PERFORMING ORGANIZATION NAME(S) AND ADDRESS(ES)

Naval Research Laboratory
4555 Overlook Avenue, SW
Washington, DC 20375-5320

8. PERFORMING ORGANIZATION REPORT NUMBER

NRL/6120/MR--2022/1

9. SPONSORING / MONITORING AGENCY NAME(S) AND ADDRESS(ES)

Naval Research Laboratory
4555 Overlook Avenue, SW
Washington, DC 20375-5320

10. SPONSOR / MONITOR'S ACRONYM(S)

NRL-NISE

11. SPONSOR / MONITOR'S REPORT NUMBER(S)

12. DISTRIBUTION / AVAILABILITY STATEMENT

DISTRIBUTION STATEMENT A: Approved for public release; distribution is unlimited.

13. SUPPLEMENTARY NOTES

*Karles Fellowship

14. ABSTRACT

The objective of this Karles Fellowship was to develop polymers stable to 400–500 °C by utilizing cyanophosphine monomers with stable, aromatic substituents. New methods have been developed to deposit thin films of thermooxidatively robust polymerized P(CN)3 that act as hard thermosets. A new method for synthesizing monocyano- and dicyanophosphines of similar structure was developed, and several of these monomers were investigated for their ability to produce robust thermosets. Phenyl dicyanophosphine (PhP(CN)2) thermosets into a hard, thermooxidatively stable, monolithic material. The novel monomer bis(diphenylamino)cyanophosphine ((Ph2N)2PCN) thermosets in a promising, waxy, black solid, but exhibits poor thermal stability due to non-oxidative intramolecular elimination reactions.

15. SUBJECT TERMS

Cyanophosphine	Phosphorus tricyanide	Synthesis
Solvothermal reactions	Thin film deposition	Polymerization

16. SECURITY CLASSIFICATION OF:			**17. LIMITATION OF ABSTRACT**	**18. NUMBER OF PAGES**	**19a. NAME OF RESPONSIBLE PERSON**
					Brian Chaloux
a. REPORT	**b. ABSTRACT**	**c. THIS PAGE**	U	38	**19b. TELEPHONE NUMBER** *(include area code)*
U	U	U			(202) 767-0819

This page intentionally left blank.

CONTENTS

This page intentionally left blank.

EXECUTIVE SUMMARY

The objective of this Karles Fellowship was to develop inorganic rubbers stable to both high temperatures (≥ 450 °C) and corrosive environments based on generalization of the chemistry of phosphorus tricyanide ($P(CN)_3$) to cyanophosphines as a general class of molecules and monomers. Previous work had shown thermosets of $P(CN)_3$ exhibited exceptional thermal stability (decomposition temperature, T_d ~ 800 °C) and chemical stability (dissolving only in hot, concentrated, oxidizing acids). Even the most robust commercial rubbers – polysiloxanes and perfluorinated polymers, such as Viton – are stable to only 300–350 °C and are prone to solvent swelling and attack by corrosive acid and / or alkali. It was desired to demonstrate that both thermosets and thermoplastics are accessible by synthesizing and polymerizing cyanophosphine monomers with varying nitrile contents.

The work performed was separated into three lines of inquiry:

A) Methods to deposit thermoset coatings directly from $P(CN)_3$.

B) Development of generally applicable syntheses to prepare (organic) R-group–substituted mono- and dicyanophosphine monomers from commercially available feedstocks.

C) Identification of cyanophosphine monomers that form thermoplastics, rather than thermosets, on polymerization, and characterization of the thermal behavior of the resulting materials.

A solvothermal growth technique was successfully developed and optimized allowing for the deposition of uniform, micron-thick films of C_3N_3P (i.e. poly–$P(CN_3)$) on glass substrates.[1] Processing $P(CN)_3$ is complicated by its dual properties that it thermosets below its measured melting point ($T_{thermoset}$ ~ 185 °C vs. T_m ~ 210 °C) and has a non-negligible vapor pressure (0.1 – 0.2 atm) at these temperatures. These difficulties were overcome by growing films from a hot solution of the monomer in a sealed, Teflon™ pressure vessel. Phosphorus tricyanide is dissolved at a 1.0 molar concentration in diphenyl ether and added to a pressure vessel under inert atmosphere along with substrates, which may be submerged either partially or entirely in the solution. Heating the sealed system for 7 days at 185 °C deposits smooth, 1–2 μm thick films on all submerged portions of the substrates (representative FIB-SEM cross-section below).

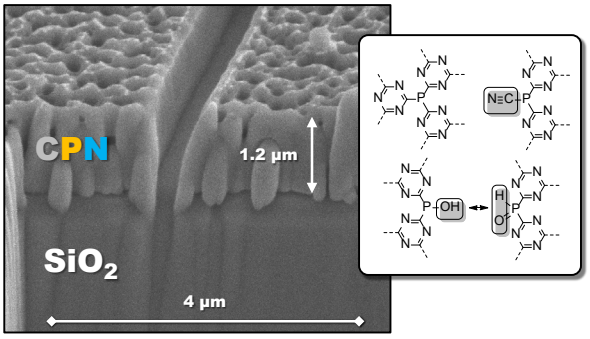

The resulting C_3N_3P films display hardness (H = 1.5 ± 0.1 GPa) and elastic modulus (E = 26.5 ± 1.5 GPa) on par with high performance engineering polymers such as Kevlar. Heat treating these films at ≥ 100 °C improves their adhesion to glass substrates without significantly affecting their physical or chemical properties (e.g. hardness, modulus, surface functional groups). These films resist decomposition to over 500 °C (above which chemistry changes and hardness increases dramatically). Although an order of magnitude softer than ultra-hard coating materials such as diamond-like carbon and plasma deposited carbon nitride films, solvothermally grown films of C_3N_3P still exhibit potential as protective coatings for a variety of applications.

Despite the attractive thermal and chemical properties of $P(CN)_3$-derived polymers, its trifunctional nature does not lend itself to the synthesis of linear, thermoplastic materials. Mono- and dicyanophosphines have been previously synthesized as (much like $P(CN)_3$) academic curiosities, but it was envisioned that these materials might polymerize into tractable, melt- or solution-processable materials while retaining some of the chemical and thermal properties of C_3N_3P. Traditional methods to prepare cyanophosphines rely on silver cyanide (AgCN) as a cyanating reagent for chlorophosphines, many of which are commercially available. Alternative reagents, such as cyanotrimethylsilane, lithium cyanide, or tetrabutylammonium cyanide are similarly expensive and inconvenient to work with. An *in situ*, one-pot (performed in the same reaction vessel without purification of intermediates), two-step method for synthesizing a diversity of mono- and dicyanophosphines from inexpensive, recyclable reagents (Figure 2) was developed to replace these traditional methods of synthesis.[2]

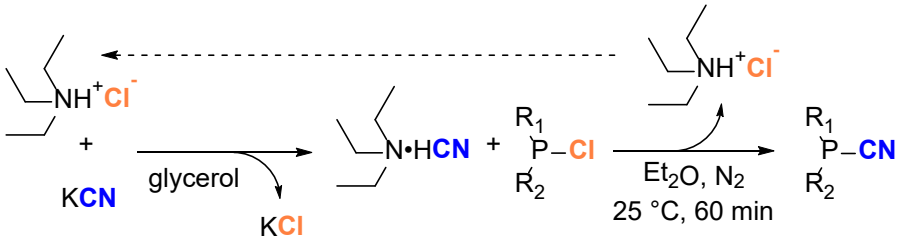

Figure 2. Reaction schematic for the use of triethylammonium chloride, KCN, and chlorophosphine to synthesize the correspond cyanophosphine. Chlorine (orange) and cyanide (blue) are highlighted to facilitate tracking the exchange of active species across steps.

Triethylammonium cyanide (TEACN), a volatile liquid prone to slow decomposition, is generated *in situ* from the reaction of potassium cyanide (KCN) and triethylammonium chloride (TEACl) in anhydrous glycerol. The TEACN is vacuum distilled onto a chlorophosphine derivative dissolved in a solvent in which TEACl is insoluble – such as diethyl ether – driving the chlorine–cyanide exchange to completion in under an hour. A series of three monocyano- and three dicyano- phosphines were prepared in moderate-to-high isolated yields (66–96%) by this method. Additionally, it was demonstrated that TEACl collected from the second step was of sufficient purity to use as-is in subsequent reactions. This synthetic methodology was shown to be generally applicable to compounds with aliphatic, aromatic, and amino side-groups.

All of the six cyanophosphines prepared in the course of developing this synthetic method were found to thermoset over a range of temperatures from 150–300 °C. All, however, formed insoluble, black solids on curing. To promote linear polymerization over cyclic trimerization of

nitriles (in hopes of making thermoplastics rather than thermosets), new aminocyanophosphine monomers with extreme steric bulk were synthesized. The synthetic protocol to prepare these two monomers of interest was ultimately optimized to a three-step, one-pot process. (Diphenylamino)dicyanophosphine ($Ph_2NP(CN)_2$) and bis(diphenylamino)cyanophosphine ($(Ph_2N)_2PCN$) were synthesized by first reacting diphenylamine with PCl_3 and triethylamine in 1,2-dimethoxyethane ('glyme'), then reacting this product with TEACN generated from KCN and TEACl as described previously (**Figure 3**).

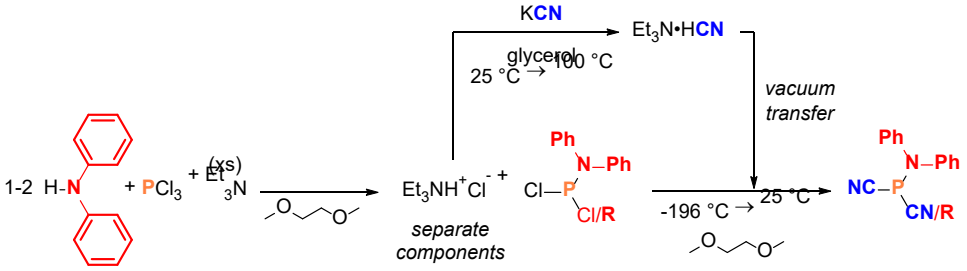

Figure 3. The synthesis of aminocyanophosphines from PCl_3, diphenylamine, and KCN by incorporating the procedure illustrated in **Figure 2**. Key components of the final product are highlighted in red (Ph_2N), orange (P), and blue (CN).

The mono–organic substituted $Ph_2NP(CN)_2$ demonstrated modest volatility (a detriment for processing) and thermoset into a brittle, black glass, much like the other cyanophosphines tested. However, $(Ph_2N)_2PCN$, bearing only one reactive CN group, instead cured over several days at 250 °C into a dark red, ductile glass. Further investigation found that the glass formed from $(Ph_2N)_2PCN$ exhibits the ability to re-melt at elevated temperature. However, the long-term thermal stability of this polymer is poor, losing 70% of its initial mass between 200° and 400 °C under inert atmosphere (Ar), transforming from a meltable glass into a hard, graphite-like solid. From Raman spectroscopy, differential scanning calorimetry (DSC, **Figure 4**), and NMR spectroscopy, the primary decomposition product from heating this material was identified as diphenylamine (Ph_2NH), implicating deleterious chemistry intrinsic to this structure (**Figure 4** inset). While this class of thermoplastic cyanophosphine-derived polymers is promising, alteration of their structure and chemistry to avoid such decomposition reactions will be necessary to realize their full potential as inorganic rubbers with good thermal stability.

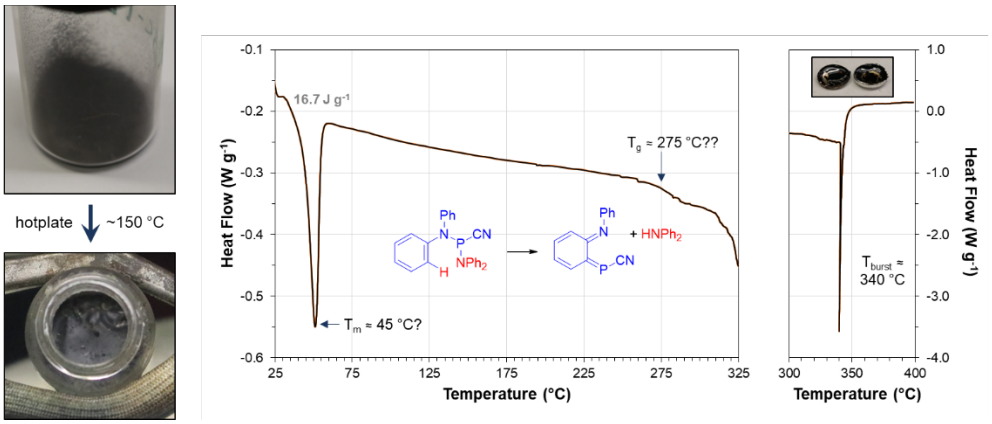

Figure 4. The melting of thermoset $(Ph_2N)_2PCN$ into a consolidated glass (left), followed by differential scanning calorimetry (DSC) showing melting of Ph_2NH crystallites, an apparent glass transition at elevated temperature (middle), and rupture of the DSC pan due to volatilization of Ph_2NH at ~340 °C (right). Speculative mechanism for elimination of Ph_2NH inset.

INORGANIC CYANOPHOSPHINE RUBBERS

Brian L. Chaloux, Code 6123

INTRODUCTION

Rubbers are invaluable components for many systems, providing flexible, air-tight connections between rigid structural elements. However, the use of rubbers in high temperature applications (e.g. combustion engines and turbines; furnaces for annealing and part post-processing; solid oxide fuel cells[3]) is restricted by the limited thermal stability of even the highest performing engineering polymers. Silicone rubbers are typically air-stable to only ~350 °C, while highly fluorinated rubbers such as Viton™ and Kalrez® are stable to ~400 °C. Additionally, continuous service temperatures are typically observed to be 50–75 °C lower than the onset of decomposition (T_d) as measured by thermogravimetric analysis (TGA).[4-7] As part of a separate program, phosphorus tricyanide ($P(CN)_3$) was discovered to quantitatively thermoset into a solid carbon phosphonitride (C_3N_3P) stable to attack by all but hot, strong, oxidizing acids (e.g. H_2SO_4:H_2O_2, HNO_3) with T_d measured at ~800 °C under both aerobic and anaerobic conditions (Figure 4).[8] It was set out to further develop the chemistry of $P(CN)_3$ for the preparation of inorganic rubbers sharing the thermal and chemical stability of C_3N_3P.

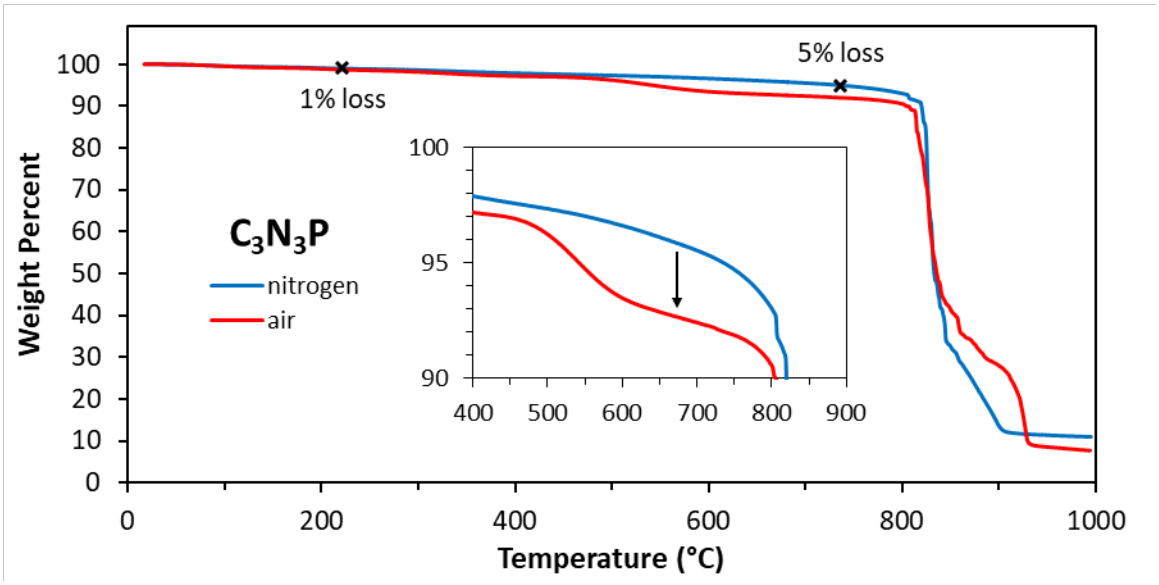

Figure 5. Thermogravimetric analysis of C_3N_3P powder under N_2 and air at a heating rate of 10 K min^{-1}. Onset of decomposition observed at 800 °C.[8]

Synthesizing rubbers from cyanophosphines requires two primary modifications to the previously-described $P(CN)_3$ system[8]: a) Transitioning to liquid reaction conditions, enabling shaped, non-porous materials; and b) Decreasing crosslink density to favor elastic, rather than brittle, thermosets[9,10]. It might be possible to decrease the crosslink density of $P(CN)_3$ thermosets by varying reaction conditions in the solid state, but it was determined that C_3N_3P powders are not amenable to powder processing at scalable temperatures and pressures (requiring ≥500 °C and ≥0.8 GPa for sintering)[11], necessitating a transition to liquid-phase polymerization conditions.

Manuscript approved January 27, 2022.

It was determined that, for this system, there are two viable methods to develop liquid-phase polymerization conditions: 1) Solution processing $P(CN)_3$; and 2) Developing alternative monomers which melt below the temperatures at which they polymerize, allowing processing while 'neat' (i.e. without solvent). Both of these methods were explored.

TECHNICAL APPROACH

Solution Processing of $P(CN)_3$

The simplest method to transition from solid to liquid reaction conditions was to develop a solvothermal system whereby $P(CN)_3$ can be polymerized in an inert solvent. A series of coordinating solvents – ethers, nitriles, and tertiary amines – were surveyed for solubility and reactivity toward $P(CN)_3$. Diphenyl ether (Ph_2O) was found to be a suitable solvent, dissolving $P(CN)_3$ at >1 molal concentration above 140 °C, boiling well above viable reaction temperatures (BP = 258 °C), showing no reactivity toward $P(CN)_3$ by nuclear magnetic resonance (NMR) spectroscopy, being comparatively inexpensive (as a perfume component), and being simple to dry and deoxygenate.

Dissolving $P(CN)_3$ allows it to polymerize under controllable conditions but does not eliminate the problem of its vapor pressure. In an unsealed system, $P(CN)_3$ will eventually be either lost from the vessel entirely or transferred to cooler parts of the vessel *via* sublimation and condensation. This necessitates a sealed, isothermal system for $P(CN)_3$ processing. Teflon™ acid digestion vessels (colloquially known as 'Parr bombs') were utilized as a reusable alternative to sealed glass ampoules. Although uneconomical to scale above ~1" substrate size in these particular vessels, any sealed, Teflon™-lined vessel that is capable of holding several bar of pressure should prove usable for scale up. Although the C_3N_3P films grown from these reactions were found to deposit on polymer (silicone), metal (copper & gold), and glass substrates of variable geometry, fused quartz slides were chosen as the substrates for the following studies due to the high quality of adhesion of C_3N_3P films.

Films grown over 7 days at 185 °C were thermally annealed at 100–550 °C to remove residual $P(CN)_3$ and solvent, then subjected to a battery of tests to characterize their chemical structure (x-ray photoelectron and infrared spectroscopies), morphology (atomic force microscopy), and physical properties (nanoindentation).

Alternative Monomer Synthesis

The films ultimately produced by solvothermal deposition of C_3N_3P onto glass from $P(CN)_3$ solutions proved to be hard and brittle, like their powder-processed analogs. This necessitated exploration of other cyanophosphine monomers for the liquid-phase synthesis of rubbery materials. Cyanophosphines with substituents (R-groups) on the phosphorus consisting of alkoxides, amines, and hydrocarbons (aliphatic and aromatic) have been previously synthesized by means analogous to the preparation of $P(CN)_3$.[12-14] However, these studies were primarily exploratory; only a single reference has explored the processing and use of cyanophosphines as precursors to polymeric materials.[15]

Developing a generally applicable means to synthesize monocyano- and dicyano- phosphines rapidly with inexpensive reagents was necessary to investigate the polymerization behavior and physical properties of a wide variety of these monomers and their resulting polymers. Prior syntheses of these materials utilized expensive cyanating reagents, such as silver and lithium cyanides (AgCN, LiCN), which in many cases take hours to react at elevated temperature due to heterogeneous reaction conditions. Although primary and secondary amines react readily with (pseudo)halophosphines (P–Cl, P–Br, P–CN groups), tertiary amines are relatively inert.[16,17]

To facilitate exchange of –CN with –Cl, HCN is generated *in situ* and combined with a suitable organic base (e.g., tertiary amine) to drive the reaction toward completion by precipitating amine hydrochloride from the reaction mixture. *In situ* generation of HCN proceeds by reaction of amine hydrochloride with KCN in a mutual, high boiling solvent, from which the vapors are transferred and condensed as the HCN–amine adduct. Different solvents were trialed for the *in situ* generation of HCN, and glycerol was found to be suitably polar and high boiling not to transfer during the vacuum distillation process. The success of the subsequent cyanide–halogen exchange reaction relies upon the differential solubility of amine hydrochloride and amine hydrogen cyanide complex in the solvent of choice. Ethereal solvents are preferable, as amine hydrochlorides are sparingly soluble therein, whereas halogenated solvents like chloroform are surprisingly good solvents for amine hydrochlorides. A series of tertiary amines including trimethylamine, triethylamine, and diisopropylethylamine (i.e. Hünig's base) were surveyed, as well as reaction solvents including diethyl ether, tetrahydrofuran, acetonitrile, dimethyoxyethane, and toluene.

The resulting cyanophosphine products were typically soluble in the reaction solvent, allowing the hydrochloride precipitate to be filtered, the reaction mixture to be concentrated, and the product to be isolated by either distillation or recrystallization. Identities of the products were confirmed by ^{1}H and ^{13}C NMR and infrared spectroscopies. New compounds ($(Ph_2N)_2PCN$) were also characterized by single crystal x-ray diffraction. Some of these compounds are liquid at room temperature and others solid at room temperature. Solids are generally thermally stable, but the liquids have the tendency to slowly decompose; to prevent this decomposition, the products were stored at -30 °C under inert atmosphere.

Assessing Cyanophosphine Thermosets

The various synthesized cyanophosphines were tested for an ability to thermoset without added catalyst by heating in capped scintillation vials on a hot plate under inert atmosphere. All of the cyanophosphines were found to convert to viscous black liquids / solids at sufficiently high temperature, although many are volatile at the temperatures at which they react. A subset of these cyanophosphines – $PhP(CN)_2$ and $(Ph_2N)_2PCN$ – was selected on which to perform more quantitative thermosetting studies.

Each of these cyanophosphines was heated to 250–300 °C in a sealed system, either a Teflon-lined pressure vessel or a flame-sealed Pyrex tube, until the colorless (liquid) monomer had set into a black solid. The solids were extracted from their reaction vessels and characterized by thermogravimetric analysis (TGA), infrared / Raman spectroscopy, and NMR spectroscopy (where components of the product were soluble in an NMR solvent).

METHODS

Synthesis

Materials were purchased from either Fisher Scientific or Sigma-Aldrich and used as received, except where otherwise noted. Solvents were either purchased anhydrous or dried prior to use. Synthetic procedures were carried out under inert atmosphere (N_2) and solvents were deoxygenated to prevent oxidation of phosphorus(III) to phosphorus(V). Diphenyl ether and 1,2-dimethoxyethane were dried and deoxygenated by distillation from Na–benzophenone ketyl. Glycerol was dried and deoxygenated by vacuum distillation after discarding the first 10% of distillate (containing residual water). Acetonitrile was dried by distillation from P_2O_5. Triethylamine hydrochloride (TEACl) and KCN were dried under vacuum prior to use. $P(CN)_3$ was freshly sublimed under vacuum at 100 °C prior to use.

$P(CN)_3$ (1a). PCl_3 (3.469 g, 25.26 mmol) and AgCN (10.487 g, 78.33 mmol) were added to 70 mL anhydrous chloroform, and the suspension was refluxed under N_2 for 16 h. Volatiles were removed from the resulting grey slurry under vacuum and the crude solid product was sublimed twice at 100 °C under dynamic vacuum, affording white, needlelike crystals in 92 % yield (2.534 g) which were qualitatively pure by NMR and vibrational spectroscopy. ^{13}C NMR (CD_3CN, 75.48 MHz): δ (ppm) = 111.67 (d, $^1J_{C\text{-}P}$ = 60.0 Hz). ^{31}P NMR (CD_3CN, 121.49 MHz): δ (ppm) = -138.71 (s + d, $^1J_{C\text{-}P}$ = 60.0 Hz). IR: ν (cm^{-1}) = 2205 m, 632 vs, 602 vs, 574 vs, 466 vw, 451 vw. Raman: ν (cm^{-1}) = 2205 vs, 632 m, 602 m, 574 m, 466 m, 451 w, 314 w, 155 s, 147 s, 119 s.

Poly-[$P(CN)_3$] on Quartz Slides (1b). Films were prepared on glossy fused quartz slides cut to dimensions of 1.5 cm × 2.5 cm × 1.5 mm. Four batches, A–D, were prepared where all samples from the same batch were simultaneously deposited in the same reactor. All slides were cleaned with soap and water, treated overnight with hot acid piranha solution (7:1 H_2SO_4 + 30% H_2O_2), rinsed with deionized (DI) water, and then dried at 185 °C prior to use. Slides were pre-scored with a glasscutter prior to cleaning to enable bisection after film deposition and analysis of fresh, identical samples by orthogonal analytical techniques.

Six (6) slides at a time were placed in a 23 mL Teflon (PTFE) cup and secured in an upright position with a notched silicone rubber bar (**Figure 6a**). 1.0 gram of $P(CN)_3$ and 10 mL preheated diphenyl ether (Ph_2O) were added to the cup. The Teflon lid was secured tightly and the closed assembly was then heated to 150 °C on a hot plate for 1 hour to dissolve the $P(CN)_3$. The cup was subsequently placed in a Parr digestion bomb (**Figure 6b**), closed tightly, and heated in a vented (to air) convection oven at 185 °C for 7 days. After deposition, the apparatus was transferred back into a dry box and disassembled. Slides were removed individually from the cup, washed with diethyl ether and THF, and gently buffed with a THF-wet Kimwipe to remove loosely adhered particulates.

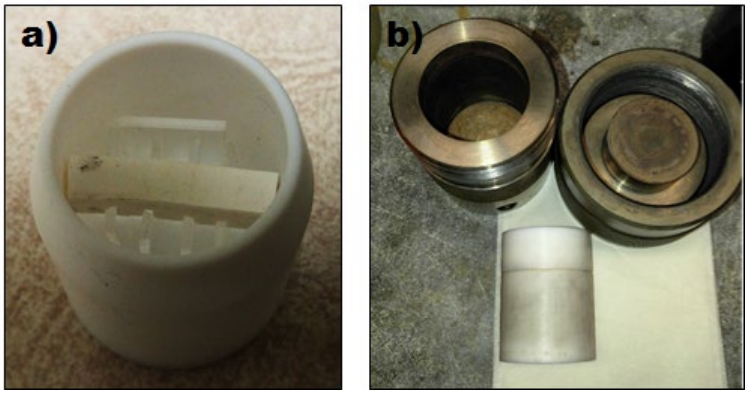

Figure 6. Apparatus for deposition of CPN films from $P(CN)_3$ solution: a) 23 mL PTFE cup with quartz slides and silicone divider; b) acid digestion bomb assembly (cup, lid, and pressure vessel).

Samples were heat treated under vacuum for 4 hours at 100 °C, 250 °C, 400 °C, or 550 °C to remove residual solvent and anneal the CPN films. The low end of heat treatment temperatures was chosen to be high enough to sublime any unreacted $P(CN)_3$ (P_{vapor} (100 °C) = 0.6 mmHg)[18] and residual Ph_2O (P_{vapor} (100 °C) = 3 mmHg). The high end of treatment temperatures was chosen to be sufficiently below the decomposition temperature of C_3N_3P measured in prior work (~800 °C at 10 °C min^{-1} heating)[8]. Sample names are abbreviated by batch letter and heat treatment temperature (e.g., D400 = Batch D, 400 °C heating).

General Method for Monocyano- and Dicyano-phosphines. In a mortar and pestle under inert atmosphere, 175 mmol (24.09 g) of triethylammonium chloride (TEACl) and 150 mmol (9.77 g) of anhydrous KCN are powdered together. The mixture is added to one side of an unfritted glass H-tube under N_2 flow along with a small magnetic stir bar and 100 mL of freshly distilled glycerol; using a glass fritted tube will prevent splatter, but slows the vacuum transfer process. The H-tube is stoppered on both sides, the receiving (empty) arm is chilled in liquid nitrogen, and the distillation (glycerol suspension) arm is gently heated in a water bath. Static vacuum is applied to the receiving side of the H-tube with care not to cause overflow in the glycerol arm. The temperature of the water bath is gradually increased until all solids have dissolved and bubbling has ceased. The H-tube is closed, pumped into a glove box, and the (solid) TEACN distillate allowed to thaw.

The colorless, liquid TEACN (~17.3 g, ~24 mL at 90% isolated yield) is transferred into a pre-weighed vial and the product massed. Under inert atmosphere, 50 mmol of chlorophosphine are dissolved in 25 mL anhydrous, deoxygenated Et_2O. A 1.1× excess of TEACN with respect to chlorine (110 mmol, 14.10 g for dichlorophosphines) is added to a round-bottom Schlenk flask equipped with an addition funnel and magnetic stirbar and dissolved in 50 mL of anhydrous Et_2O. The solution of chlorophosphine is transferred to the addition funnel and added dropwise to the solution of TEACN while stirring rapidly. White, crystalline solids (TEACl) precipitate and the solution (typically) turns yellow in color. The solution is stirred for an additional 30 minutes after addition has completed. Solids are filtered off from the solution by suction filtration, the filtrate transferred to a fresh round-bottom Schlenk flask, and volatiles removed under vacuum to recover

cyanophosphine product. The resulting cyanophosphines are purified by either vacuum distillation or recrystallization.

Phenyldicyanophosphine (2a). Ground 7.069 g (108.6 mmol) KCN with 14.994 g (108.9 mmol) and transferred powder to distillation arm of an H-tube along with a magnetic stirbar. While flushing with N_2, added 75 mL glycerol to the distillation arm and chilled the receiving arm in LN_2. Closed distillation arm, pulled vacuum through receiving arm, and heated distillation arm to 80 °C in a water bath. Isolated 12.306 g (42.79 mmol) TEACN distillate (39% yield) after vacuum distillation and thawing.

Transferred a magnetic stirbar and the entire portion of TEACN (42.79 mmol) to a round-bottom flask, dissolving in 15 mL Et_2O. Attached an addition funnel and added 2.64 mL (19.5 mmol) phenyldichlorophosphine and 20 mL Et_2O to the funnel. Added phosphine solution dropwise to the stirring TEACN solution, suction filtered off the solids in a glass fritted filter funnel, then concentrated filtrate under vacuum, isolating 2.850 g pale yellow oil. Vacuum distilled crude product, collecting 1.964 g colorless oil (63% isolated yield); the oil is prone to crystallization when transferring via pipet, but can remain a super-cooled liquid for extended periods. ^{1}H NMR ($CDCl_3$, 300.13 MHz): δ (ppm) = 7.80 (m, 2H), 7.59 (m, 1H), 7.50 (m, 2H). ^{13}C NMR ($CDCl_3$, 75.48 MHz): δ (ppm) = 134.45 (d, $^{1}J_{P\text{-}C}$ = 25.9 Hz), 133.06 (s), 129.73 (d, $^{2}J_{P\text{-}C}$ = 10.3 Hz), 116.09 (d, $^{1}J_{P\text{-}C}$ = 439.7 Hz), 113.98 (s). ^{31}P NMR ($CDCl_3$, 121.49 MHz): δ (ppm) = -72.53 (s). IR: see **Figure 7**.

Diphenylcyanophosphine (3). Ground 5.190 g (79.7 mmol) KCN with 10.953 g (79.6 mmol) TEACl and transferred to distillation arm of an H-tube along with a magnetic stirbar. While flushing with N_2, added 50 mL glycerol to the distillation arm and chilled the receiving arm in LN_2. Closed distillation arm, pulled vacuum through receiving arm, and heated distillation arm to 80 °C in a water bath. Collected 8.819 g (35.04 mmol) TEACN distillate (49% isolated yield) after vacuum distillation and thawing.

Transferred a magnetic stirbar and the entire portion of TEACN (35.04 mmol) to a round-bottom flask, dissolving in 20 mL Et_2O. Attached an addition funnel and added 5.837 mL (31.85 mmol) diphenylchlorophosphine and 20 mL Et_2O to the funnel. Added phosphine solution dropwise to the stirring TEACN solution, suction filtered off solids in a glass fritted filter funnel, then concentrated filtrate under vacuum, isolating 6.584 g yellow oil. Vacuum distilled crude product, isolating 5.448 g (81% yield) colorless liquid. ^{1}H NMR ($CDCl_3$, 300.13 MHz): δ (ppm) = 7.50 (m, 4H), 7.33 (m, 6H). ^{31}P NMR ($CDCl_3$, 121.49 MHz): δ (ppm) = -32.91 (quintet, $^{3}J_{H\text{-}P}$ = 8.9 Hz). IR: see **Figure 7**.

Cyclohexyldicyanophosphine (4). Ground 3.013 g (46.27 mmol) KCN with 6.376 g (46.32 mmol) TEACl and transferred to distillation arm of an H-tube along with a magnetic stirbar. While flushing with N_2, added 30 mL of glycerol to the distillation arm and chilled the receiving arm in LN_2. Closed distillation arm, pulled vacuum through receiving arm, and heated distillation arm to 80 °C in a water bath. Collected 3.097 g (24.15 mmol) TEACN distillate (52% isolated yield) after vacuum distillation and thawing.

Transferred a magnetic stirbar and 1.302 g (10.16 mmol) TEACN to a round-bottom flask, dissolving in 10 mL Et_2O. Attached an addition funnel and added 0.83 mL (5.40 mmol)

cyclohexyldichlorophosphine and 10 mL Et_2O to the funnel. Added phosphine solution dropwise to the stirring TEACN solution, suction filtered off solids in a glass fritted filter funnel, then concentrated filtrate under vacuum, isolating 0.808 g (90% yield) colorless oil. ^{31}P NMR ($CDCl_3$, 121.49 MHz): δ (ppm) = -58.10 (m). IR: see **Figure 7**.

Dicyclohexylcyanophosphine (5). Ground 1.4094 g (21.64 mmol) KCN with 2.9473 g (21.41 mmol) TEACl and transferred to distillation arm of an H-tube along with a magnetic stirbar. While flushing with N_2, added 25 mL glycerol to the distillation arm and chilled the receiving arm in LN_2. Closed distillation arm, pulled vacuum through receiving arm, and heated the distillation arm to 80 °C in a water bath. Collected 2.3877 g (7.268 mmol) TEACN distillate (34% isolated yield) after vacuum distillation and thawing.

Transferred a magnetic stirbar and entirety of collected TEACN (7.268 mmol) to a round-bottom flask, dissolving in 10 mL Et_2O. Attached an addition funnel and added 0.95 mL (4.30 mmol) dicyclohexylchlorophosphine and 10 mL Et_2O to the funnel. Added the phosphine solution dropwise to the rapidly-stirring TEACN solution, suction filtered off solids in a glass fritted filter funnel, then concentrated filtrate under vacuum, isolating 0.7037 g (73% yield) of colorless oil. ^{1}H NMR ($CDCl_3$, 300.13 MHz): δ (ppm) = 1.8–1.4 (m, 10H), 1.2–0.9 (m, 12H). ^{13}C NMR ($CDCl_3$, 75.48 MHz): δ (ppm) = 121.40 (d, $^{1}J_{C\text{-}P}$ = 77.9 Hz), 31.46 (d, $^{n}J_{C\text{-}P}$ = 10.4 Hz), 29.79 (d, $^{n}J_{C\text{-}P}$ = 9.9 Hz), 29.70 (d, $^{n}J_{C\text{-}P}$ = 11.5 Hz), 26.58 (d, $^{n}J_{C\text{-}P}$ = 20.9 Hz), 26.17 (d, $^{n}J_{C\text{-}P}$ = 53.8 Hz). ^{31}P NMR ($CDCl_3$, 121.49 MHz): δ (ppm) = -16.98 (m). IR: see **Figure 7**.

(Diethylamino)dicyanophosphine (6). Ground 8.199 g (125.9 mmol) with 17.296 g (125.7 mmol) TEACl and transferred to distillation arm of an H-tube along with a magnetic stirbar. While flushing with N_2, added 100 mL glycerol to the distillation arm and chilled the receiving arm in LN_2. Closed distillation arm, pulled vacuum through receiving arm, and heated distillation arm to 80 °C in a water bath. Collected 8.644 g (38.63 mmol) TEACN distillation (31% isolated yield) after vacuum distillation and thawing.

Transferred a magnetic stirbar and entirety of collected TEACN (38.63 mmol) to a round-bottom flask, dissolving in 50 mL Et_2O. Attached an addition funnel and added 2.55 mL (17.6 mmol) (diethylamino)dichlorophosphine and 25 mL Et_2O to the funnel. Added the phosphine solution dropwise to the rapidly-stirring TEACN solution, suction filtered off solids in a glass fritted filter funnel, then concentrated filtrate under vacuum, isolating 2.256 g (83% yield) of yellow oil. ^{1}H NMR ($CDCl_3$, 300.13 MHz): δ (ppm) = 3.15 (dq, $^{3}J_{H\text{-}H}$ = 7.4 Hz, $^{3}J_{P\text{-}H}$ = 13.4 Hz, 4H), 1.12 (t, $^{3}J_{H\text{-}H}$ = 7.4 Hz, 6H). ^{31}P NMR ($CDCl_3$, 121.49 MHz): δ (ppm) = -12.96 (quintet, $^{3}J_{H\text{-}P}$ = 13.4 Hz). IR: see **Figure 7**.

Bis(diethylamino)cyanophosphine (7). Ground 3.5097 g (53.90 mmol) KCN with 7.4048 g (53.79 mmol) TEACl and transferred to distillation arm of an H-tube along with a magnetic stirbar. While flushing with N_2, added 50 mL glycerol to the distillation arm and chilled the receiving arm in LN_2. Closed distillation arm, pulled vacuum through receiving arm, and heated distillation arm to 80 °C in a water bath. Collected 6.178 g (48.18 mmol) TEACN distillate (90% isolated yield) after vacuum distillation and thawing.

Transferred a magnetic stirbar and 4.525 g (35.29 mmol) TEACN to a round-bottom flask, dissolving in 50 mL Et_2O. Attached an addition funnel and added 3.36 mL (15.98 mmol)

bis(diethylamino)chlorophosphines and 25 mL Et_2O to the funnel. Added phosphine solution dropwise to the rapidly-stirring TEACN solution, suction filtered off solids in a glass fritted filter funnel, then concentrated filtrate under vacuum. The crude product was transferred to a small H-tube and vacuum distilled, isolating 4.252 g of product as a colorless oil (89% isolated yield). ^{1}H NMR ($CDCl_3$, 300.13 MHz): δ (ppm) = 2.99 (m, 8H), 0.91 (t, $^{3}J_{H\text{-}H}$ = 7.2 Hz, 12H). ^{13}C NMR ($CDCl_3$, 75.48 MHz): δ (ppm) = 122.07 (d, $^{1}J_{P\text{-}C}$ = 61.6 Hz), 43.87 (d, $^{2}J_{P\text{-}C}$ = 18.9 Hz), 14.08 (d, $^{3}J_{P\text{-}C}$ = 3.7 Hz). ^{31}P NMR ($CDCl_3$, 121.49 MHz): δ (ppm) = 57.40 (m, $^{3}J_{H\text{-}P}$ = 9.0 Hz). IR: see **Figure 7**.

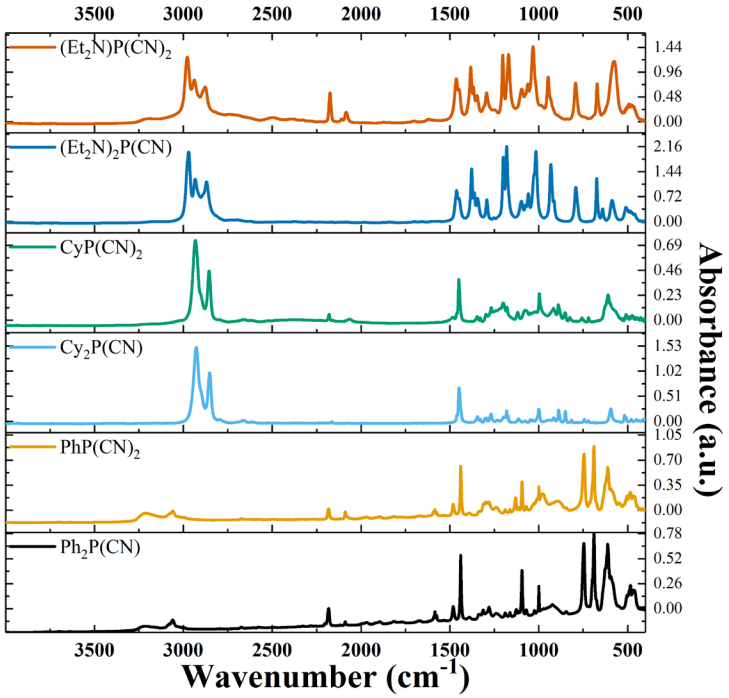

Figure 7. Infrared spectra of cyanophosphine monomers **2-7** obtained on a diamond ATR crystal.

Bis(diphenylamino)cyanophosphine (8a). A portion of triethylamine (TEA) was dried by passing through an activated alumina column. Added a magnetic stir bar, 6.42 g (37.9 mmol) diphenylamine, 7.0 mL (50 mmol) dry TEA, and 50 mL anhydrous 1,2-dimethoxyethane (DME) to one arm of a glass-fritted H-tube; the solution was freeze–pump–thaw cycled to deoxygenate. Added 1.80 mL (20.6 mmol) PCl_3 via syringe, closed the solution arm of the H-tube, then heated solution to reflux with the empty arm open to N_2. Reaction progress was periodically monitored by taking aliquots into $CDCl_3$ for ^{31}P NMR. After 5 days, reaction had completed (>10:1 ratio of $(Ph_2N)_2PCl$ to $(Ph_2N)PCl_2$ by ^{31}P NMR, with no PCl_3 remaining) and the product was suction filtered into the receiving side of the H-tube. The filtrand (primarily TEACl) was washed several times with 10 mL portions of anhydrous DME and was subsequently tapped back into the bulb of the H-tube.

To the crude TEACl filtrand (~38 mmol), 1.95 g (29.9 mmol) powdered KCN and 50 mL anhydrous glycerol were added. The filtrate from the previous step was chilled in LN_2. The suspension of KCN and TEACl in glycerol was heated gently in a water bath and vacuum pulled through the filtrate arm of the H-tube. The bath temperature was gradually heated over a period of

2 hours, after which bubbling had ceased and solids had completely dissolved. N_2 was re-introduced to the H-tube and the TEACN + $(Ph_2N)_2PCl$ + DME mixture allowed to warm to room temperature. The yellow-orange solution was stirred for 16 hours, over which white solids precipitated.

In a glovebox, the glycerol solution removed and the (now) empty arm rinsed with diethyl ether. The DME solution was suction filtered into the clean, empty arm to remove precipitated TEACl. The filtrand was washed several times with 10 mL portions of DME, then volatiles were removed from both filtrate and filtrand under vacuum. The product (filtrate) was collected as an off-white, waxy solid (6.20 g, 76% isolated yield). Crystals suitable for x-ray crystallography were grown by slow cooling a hot, saturated solution of product in diethyl ether to room temperature. ^{1}H NMR ($CDCl_3$, 400.13 MHz): δ (ppm) = 7.32 (t, $^3J_{H-H}$ = 7.7 Hz, 8H), 7.21 (t, $^3J_{H-H}$ = 7.2 Hz, 4H), 7.08 (d, $^3J_{H-H}$ = 8.1 Hz, 8H). ^{13}C NMR ($CDCl_3$, 100.61 MHz): δ (ppm) = 145.96 (d, $^2J_{P-C}$ = 11.4 Hz), 129.38 (s), 125.09 (d, $^3J_{P-C}$ = 3.1 Hz), 125.00 (s), 120.56 (d, $^1J_{P-C}$ = 71.0 Hz). ^{31}P NMR ($CDCl_3$, 161.98 MHz): δ (ppm) = 52.15 (s). The crystal structure obtained as detailed in **Methods: Characterization** is illustrated in **Figure 8** and its parameters detailed in **Table 1**, below.

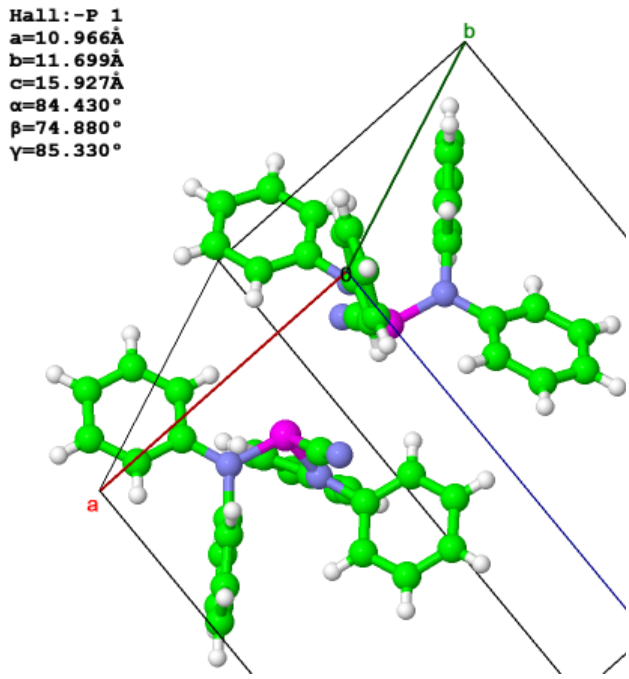

Figure 8. Unit cell of $(Ph_2N)_2PCN$ (**8a**)

Table 1. Crystal structural parameters of $(Ph_2N)_2PCN$ (**8a**)

8a	
Formula	$((C_6H_5)_2N)_2PCN$
Formula Weight	393.41
Crystal System	Triclinic
Space Group	P
a (Å)	10.966(2)
b (Å)	11.699(2)
c (Å)	15.927(3)
α (°)	84.43(3)
β (°)	74.88(3)
γ (°)	85.33(3)
Vol (Å^3)	1959.9(7)
Z	4
ρ (g cm^{-3})	1.333
μ (mm^{-1})	0.157
R_{int}	0.0623
R_1	0.0410
wR_2	0.0936

Poly-[PhP(CN)$_2$] (2b). In a nitrogen-filled glovebox, a small quartz crucible was placed into a Teflon acid digestion cup and 1.0 mL $Ph_2P(CN)_2$ (**2a**) added to the crucible. The assembly was sealed, placed into a Parr acid digestion bomb, and heated to 250 °C for 60 hours. The assembly was subsequently removed from the oven, returned to the glovebox, and the quartz crucible removed from the Teflon cup. The cap of the cup was covered in hard, black beads of solid, while

the crucible was filled with a smooth, monolithic, solid puck. The puck was removed from the crucible by cooling in liquid nitrogen, causing it to fracture into multiple large pieces.

Poly-[$(Ph_2N)_2PCN$] (8b). 1.021 g (2.595 mmol) freshly recrystallized $(Ph_2N)_2PCN$ (**8a**) powder were added to a thick-walled, 5 mm ID Pyrex tube, which was subsequently flame sealed under vacuum. The tube was placed in a box furnace and ramped from 150 °C to 350 °C at a rate of 30 °C per hour. Fusion of the solids was observed at ~160 °C, with darkening from pearl to orange observed at ~200 °C. After holding at 350 °C for 10 hours, the product remained a black liquid. The tube was subsequently cooled to room temperature, transferred to a glovebox, and 0.760 g black solids (74% isolated yield) extracted from the tube using a drill bit.

Characterization

Nuclear magnetic resonance (NMR) spectra of soluble products were collected on either a Bruker AVANCE 300 MHz (^1H) spectrometer or a Bruker AVANCE NEO 400 MHz (^1H) spectrometer using either $CDCl_3$ or CD_3CN as the deuterated solvent. Infrared spectra were acquired in attenuated total internal reflectance (ATR) geometry on a single-bounce diamond ATR crystal using a Nicolet iS50 infrared spectrometer. Raman spectra were collected on a Renishaw inVia confocal Raman microscope using an argon ion laser operating at 514 nm.

X-ray photoelectron spectra (XPS) were collected on a Thermo Scientific K-Alpha XPS; binding energies were calibrated to adventitious carbon (C1s = 284.8 eV) and spectra fit with Shirley backgrounds and symmetrical Gaussian–Lorentzian (GL) peaks. X-ray diffraction (XRD) was performed in grazing incidence mode (0.2° incident angle) on a Rigaku SmartLab diffractometer using Cu Kα radiation. Powder x-ray diffraction (PXRD) data was performed on a Rigaku SmartLab powder diffractometer using Cu K_α radiation. Grazing incidence x-ray diffraction (GIXRD) was performed at a 0.2° incident angle on a Rigaku SmartLab powder diffractometer using Cu K_α radiation.

Single crystal x-ray diffraction (SCXRD) was performed on a Bruker D8 Quest diffractometer equipped with a Photon II detector using Mo K_α (λ = 0.71073 Å) radiation at 100 K. Samples were mounted onto a MiTeGen MicroMount™ with vacuum grease. Crystal structures were solved with intrinsic phasing using ShelXT21 and were refined using SHELX2018-122 contained within the APEX III suite of programs. All non-hydrogen atoms were located via difference Fourier maps and refined anisotropically; all hydrogen atoms on carbon atoms were placed at their idealized positions and allowed to ride on the coordinates of their parent atoms (Uiso fixed at 1.2Ueq).

Thermogravimetric analysis (TGA) was performed in alumina crucibles on a Netzsch STA 449 F1 Jupiter thermal gravimetric analyzer at a heating rate of 10 °C / min under either argon or a simulated air (20% O_2 in Ar balance) environment. Differential scanning calorimetry (DSC) was performed in aluminum pans on a TA Instruments Q100 differential scanning calorimeter under N_2 atmosphere at a heating rate of 20 °C / min.

Scanning electron microscopy (SEM) was performed on a Zeiss Leo SEM and FIB performed on a FEI Nova 600 NanoLab SEM, both operating at 5 keV. AFM images were acquired with an Asylum Cypher AFM operated in contact mode. Nanoindentation measurements were made with a Hysitron Ubi instrumented indenter operated in load control configuration. A diamond indenter of Berkovich pyramidal geometry was impressed to peak loads of 100, 500, and 1000 μN at 5 second loading and unloading rates with a hold time at peak load of 5 seconds. The unloading

curves were analyzed using the Oliver and Pharr method[19] to determine reduced modulus (E_r) and hardness (H).

RESULTS AND DISCUSSION

Carbon Phosphonitride Coatings from $P(CN)_3$

Major challenges with using $P(CN)_3$ as a precursor to high temperature thermosets are the various difficulties in its processing. To overcome these difficulties, a solvothermal method has been developed allowing deposition of flat (5–20 nm RMS surface roughness at 1 μm^2; Figure 7, Table 1), non-macro/meso-porous films of carbon phosphonitride (CPN) in the thickness range of 1–2 μm over the course or several days. Utilizing a sealed apparatus (**Figure 6**) was crucial to prevent loss of $P(CN)_3$ monomer under deposition conditions. Diphenyl ether (Ph_2O) was found to be an ideal solvent, combining sufficiently low vapor pressure (~110 mmHg at 185 °C), dissolution power for $P(CN)_3$ (≥1 molal at 140 °C), and inertness to the reactive monomer. Not shown here, ^1H and ^{13}C NMR spectra confirmed that Ph_2O remains unreacted after heating with $P(CN)_3$ to 185 C for 16+ hours; at the concentrations of $P(CN)_3$ used (1 molal), there is only a 6:1 ratio of solvent to $P(CN)_3$, so any reaction of solvent with solute should be apparent.

Film Morphology

Although films grow with low surface roughness compared to overall film thickness, a substantial number of micron-sized particulate dot the surface of all CPN films that were characterized. Surface coverage of these particles was low, but non-negligible. However, their presence suggests that the film growth process is of a sol-gel type: reactions of $P(CN)_3$ in solution generate intermediates which eventually fall out of solution and act as nucleation sites for further growth. Sol-gel behavior was also observed qualitatively in NMR scale test reactions (not shown): given several days reaction time, black gels formed within the 4 mm inner diameter tubes. The most marked difference between the growth of CPN and an analogous solvothermal deposition of *g*-C_3N_4 from acetonitrile[20] is film morphology. While Xie *et alia*'s solvothermally grown *g*-C_3N_4 films appear to be compacts of bumpy 1–5 μm diameter particles[20], the building blocks of CPN films grown from $P(CN)_3$ in Ph_2O appear by AFM (**Figure 9**) to be closer to tens of nanometers in size.

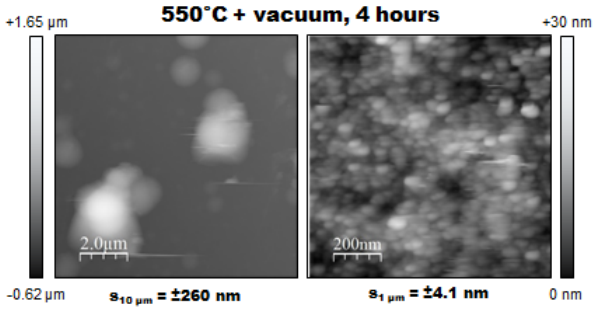

Figure 9. Representative height maps of CPN film on fused quarts (550 °C treatment, Batch A) on large (10 μm × 10 μm, left) and small (1 μm × 1 μm, right) length scales. Particles visible in SEM (**Figure 10**) also show up clearly in the lefthand AFM image.

To obtain a qualitative picture of film morphology and roughness, select samples were sputter coated with 10 nm of gold (to prevent charging) and imaged at 5 keV on an SEM. **Figure 10** shows representative images for CPN films from Batch A heat treated at various temperatures acquired at 1000× zoom. All samples are speckled with particulate 1–5 μm in diameter, but film surfaces are otherwise smooth and appear to change little with increasing temperature of heat treatment. Aside from mud-flat type cracking observed at lower anneal temperatures, the films do not appear to be macroporous.

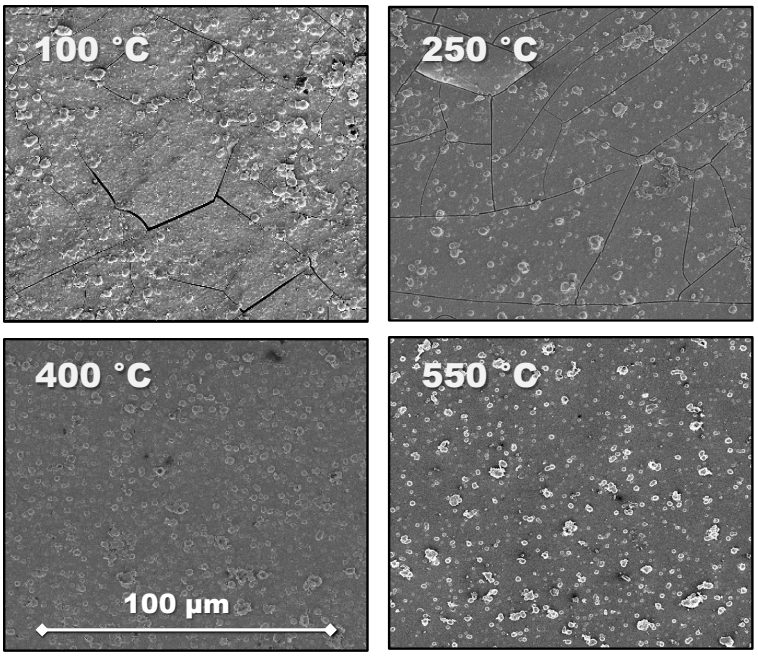

Figure 10. SEM images of CPN films on fused quartz (Batch A) at various temperature of heat treatment. 100 °C and 250 °C treated films exhibit mud-flat type cracking due to shrinkage; all films are dotted with surface particulate. All images to same scale (1,000× magnification).

Using previously acquired AFM images, the surface roughness of the solvothermally grown CPN films was subsequently assessed as a function of heat treatment temperatures and at different length scales. **Table 2** summarizes RMS surface roughness results from these data. On a lateral (x-y) scale of 1 μm, small enough to avoid inclusion of particulate, surface roughness on the order of ±5–20 nm was calculated, decreasing slightly with increasing heat treatment temperature. At larger lateral scales of 10 μm, surface roughness increases to ~100 nm, likely due to the 1–5 μm particles decorating the film surface. High-resolution AFM topographical maps show texture, but a distinctive morphology is not immediately apparent from these images.

Table 2. RMS roughness of CPN films calculated from AFM height maps

	A100	**A250**	**A400**	**A550**
10 × 10 μm	**120 nm**	**170 nm**	**31 nm**	**260 nm**
1 × 1 μm	**22 nm**	**9.1 nm**	**4.6 nm**	**4.1 nm**

To determine whether the measured surface roughness contributes significantly to the variance in film thickness, thicknesses were measured by milling a 8 μm × 8 μm square region with a focused gallium ion beam (FIB) and imaging the cross-sections *in situ* at a tilt angle of 52°. SEM images of FIB-milled regions from Batch A are shown in **Figure 11**.

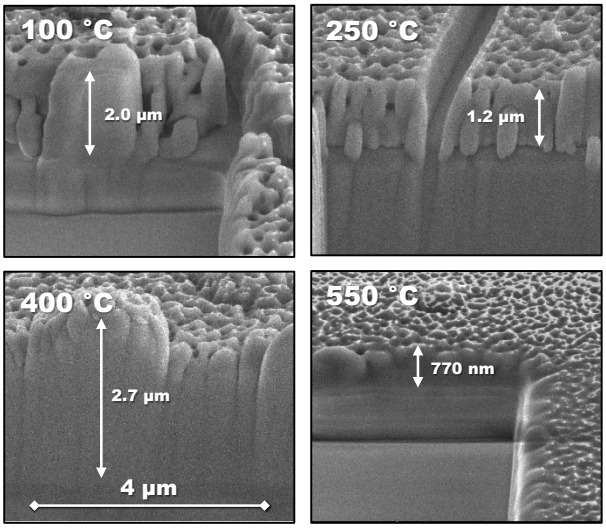

Figure 11. SEM of film cross-sections after ion milling to expose interior and substrate, acquired at 52° tilt. Pockmarking and vertical striations result from ion exposure and cannot be attributed to morphology. Cracks in top images result from 'mud-flat' cracking seen in **Figure 10**.

CPN films were distinct in SEM from the underlying fused quartz substrates. Side-on profiles, particularly of mud-flat type cracks, showed no visible macro- or mesoporosity. This does not preclude microporosity due to nanoparticle packing or included solvent, which cannot be ascertained from the SEM data as the pixel size for these images (25,000× magnification) is ~6 nm. Although film surfaces appear pockmarked in **Figure 10**, pockmarking is a result of gallium ion bombardment and is not visible in pristine regions of the film. Likewise, vertical striations cannot be unambiguously assigned to a columnar growth pattern, as ion milling does not produce a clean edge[21]; mud-flat cracks visible in **Figure 10** show little morphology viewed edge-on.

Batch A films ranged from 700 nm thick in the lower limit to 2.7 μm thick in the upper limit, but showed no clear trends in thickness versus anneal temperature. Batch D films were less varied in thickness, ranging from 0.8 μm to 1.0 μm. Sample A550 was also analyzed by grazing incidence X-ray diffraction to determine whether any crystallization occurs at increased heat treatment temperature; neither substrate nor film displays any crystallinity even after annealing at 550 °C for 4 hours.

Film Chemistry

To evaluate differences in chemistry between solvothermally grown CPN films and neat C_3N_3P powder, X-ray photoelectron spectra (XPS), energy dispersive x-ray spectra (EDS), and infrared spectra (IR) were acquired for films and compared to XPS, bulk elemental analysis, and IR previously reported for C_3N_3P.[8] Tabulated elemental compositions for Batch A (XPS) and Batch D (EDS) are given in **Table 3**, below.

Table 3. Representative compositional analysis by XPS and SEM-EDS

Technique	Sample	Composition (atomic %)				
		C	N	P	O	Si
XPS	A250	45.1	15.9	11.2	27.2	0.6
	A400	45.5	13.4	11.7	27.8	1.5
	A550	59.6	12.4	6.3	19.1	1.6
EDS	D100	49.1	16.9	9.2	23.8	1.0
	D250	53.4	17.6	6.7	21.6	0.8
	D400	47.3	14.4	8.6	28.6	1.2
	D550	53.1	12.0	9.8	23.6	1.5

Although calculated atomic percentages for C, N, P, O, and Si vary slightly sample-to-sample, overall results are consistent between XPS and EDS, showing similar surface and bulk compositions. The expected elemental make-up of C_3N_3P is C = 43 at. %, N = 43 at. %, P = 14 at. %, which is approximately the value found (when converted from wt. %) for $P(CN)_3$ polymerized neat.[8] CPN films grown from Ph_2O, however, were found to contain a substantial amount of oxygen (22–28 at. %) and a significantly reduced amount of nitrogen (12–18 at. %). The low silicon content (<2 at. %) likely arises from the substrate or silicone bar holding the samples. However, silicon incorporation of up to 2 at. % Si is insufficient to account for the oxygen introduced, regardless of whether the silicon originates from the substrate or the holding bar. The *in situ* nuclear magnetic resonance (NMR) of 1.0 molal $P(CN)_3$ in Ph_2O showed conclusively that diphenyl ether was inert to $P(CN)_3$ at 185 °C. Reaction with diphenyl ether therefore cannot be the source of oxygen in the product. However, diphenyl ether trapped in micropores may account for some, but not all, of the oxygen in the films.

Despite substantial differences in elemental composition for the CPN films and C_3N_3P powder, XPS spectra (peak locations and intensities) of P2p and N1s (**Figure 12**) regions appear remarkably similar. When annealing films to 550 °C, P2p spectra appear almost identical to C_3N_3P powder, save a small, high binding energy peak that appears at 138–139 eV. N1s spectra differ more substantially versus temperature, but can be fit consistently with two peaks, one centered at ~399 eV, which remains approximately invariant, the other shifting to higher binding energy at higher anneal temperatures. O1s spectra, likewise, can be fit with two peaks at 531 eV and 533 eV, with intensities varying with sample. C1s spectra, unlike P2p, N1s, and O1s spectra, appear to differ substantially between C_3N_3P powders and solvothermally grown CPN films. Two major components, at 285 eV and 287 eV, are present in both materials, while the high binding energy shoulder at 288 eV shows only in C_3N_3P. As powders were manipulated under air prior to XPS, this shoulder is likely attributable to some form of surface oxidation.

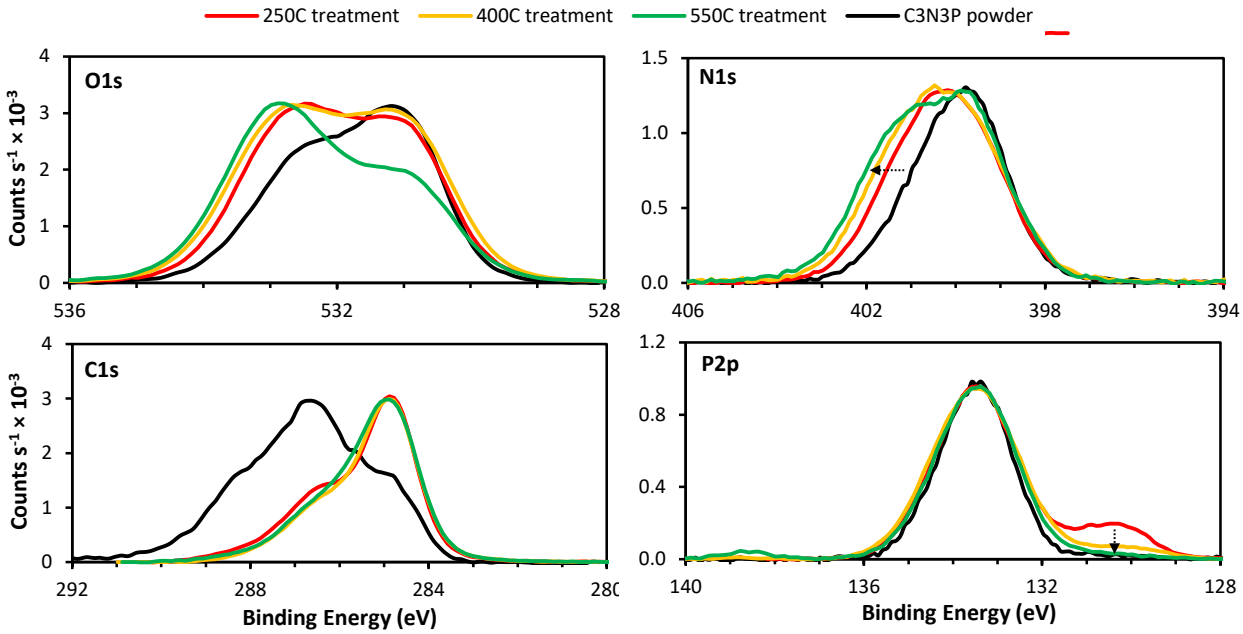

Figure 12. Overlaid comparisons of O1s, N1s, C1s, and P2p XPS spectral regions for C_3N_3P powder and Batch A films heat treated at 250 °C, 400 °C, and 550 °C. Shirley backgrounds subtracted, normalized to lowest peak intensity.

Infrared spectra of CPN films from Batch A obtained by the ATR method provide complementary structural data to XPS spectra of the same. The ATR-IR spectrum of sample A1 is shown in **Figure 13** with tentative peak assignments for the CPN film provided in **Table 4**. Film thicknesses (1–2 μm, **Figure 11**) are of an order of magnitude comparable to the evanescent wave depth of the ATR probe[22], thus SiO_2 substrate peaks are also observed in the spectra of Batch A films. Like C_3N_3P, no sharp features due to the CPN film are resolvable. Despite substantial differences in elemental composition, XPS and IR spectra show similarities in the types of moieties present between solvothermally grown CPN and C_3N_3P. In light of the XPS and EDS data available for Batches A and D and better signal-to-noise in the CPN films compared to prior analysis of C_3N_3P powders by ATR-IR, peak assignments have been tentatively assigned for both films and powders. The broad peak from 3600 – 2500 cm^{-1} is assigned to O-H stretching, the peak at ~2400 cm^{-1} to P-H stretching, and the peak at 2200 cm^{-1} to C≡N stretching. Peaks from 1700 – 700 cm^{-1} can be largely assigned to aromatic ring modes, with P=O stretching at 1190 cm^{-1} (asymmetric) and 1050 cm-1 (symmetric) and broad, overlaid peaks for Si-O stretching modes from 1300 – 1000 cm^{-1} and at 800 cm^{-1} (see **Table 4**).

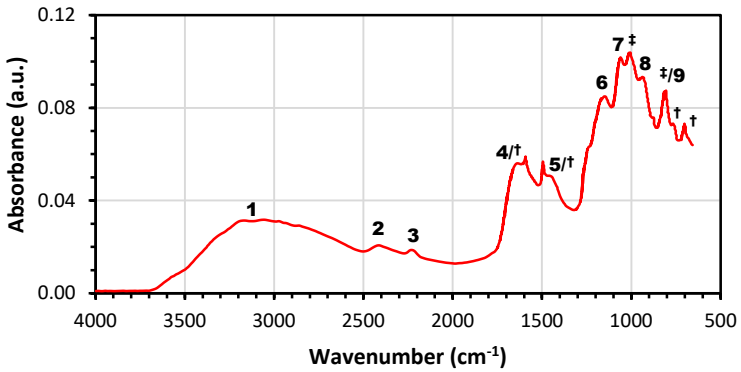

Figure 13. ATR-IR spectrum of sample A100 with peaks labeled according to assignments from Table 2. Contributions from diphenyl ether (Ph_2O) are marked with † and from underlying SiO_2 substrate marked with ‡.

Table 4. IR peak assignments for CPN films

#	v (cm^{-1})	mode(s)
1	**3600 - 2500**	**O-H stretch**
2	**2400**	**P-H stretch**
3	**2200**	**C≡N stretch**
4	**1560**	**Quadrant stretch**
5	**1420**	**Semi-circle stretch**
6+7	**1190, 1050**	**P=O stretch**
8	**950**	**Semi-circle stretch + P-H bend + P-O stretch**
9	**820**	**Sextant out-of-plane bend + P-H rock**

When heat treated, three major changes are noted in IR spectra: 1) discrete molecular peaks for diphenyl ether disappear; 2) P-H and C≡N vibrational modes disappear, while P=O intensity increases; and 3) at the highest temperatures, the P=O stretching modes broaden and shift to higher frequency. These details are illustrated in **Figure 15**.

The primary quandary arising from the characterization of our solvothermally grown CPN films is the substantial difference in elemental composition – particularly nitrogen and oxygen content – from the expected values (C = 43 at. %, N = 43 at. %, and P = 14 at. % for $P(CN)_3$ and C_3N_3P). Assaying for only 12–18 at. % nitrogen and 22–28 at. % oxygen, it might be reasonable to assume that metathesis of these elements occurs between $P(CN)_3$ and Ph_2O over the course of the reaction. Although Ph_2O and Ph_3N share similar enough ^1H NMR spectra that they might be indistinguishable for concentrated samples, ^{13}C NMR differ enough that they should clearly resolve formation of Ph_3N. No changes in the ^{13}C spectra were observed over 4 days of NMR scale reaction, disproving this hypothesis about the origin of oxygen in our CPN films. At a 1.0 molal concentration of $P(CN)_3$, there are only 6 molar equivalents of Ph_2O, so any changes observed in elemental analyses should also be observable by ^{13}C (and ^1H) NMR.

Ph_2O trapped in micropores could skew both carbon and oxygen content high, but can only account for 3–5 at. % oxygen based on the amount of carbon present. Alternative explanations rely on the unplanned introduction of oxygen into the reaction mixture, either in the form of O_2 or H_2O. Although the vast majority of manipulations took place in a glove box, the sealed digestion bomb used for the solvothermal growth step was taken out into air for heating in an oven.

IR spectra help narrow down the mechanism of oxygen inclusion in CPN films (and, in retrospect, in C_3N_3P powders). Initially, the broad peak from 3600 – 2500 cm^{-1} in both films (**Figure 13**) and C_3N_3P powder[8] was assigned to aromatic overtones and combination bands of the 1700 cm^{-1} – 1200 cm^{-1} region (predominantly ring modes). Although such an assignment is plausible, vapor-deposited C_3N_4 films, which demonstrate similar ring modes from 1700 cm^{-1} – 1200 cm^{-1}, show no absorbance at >2300 cm^{-1}, *except* for the melamine-derived samples which assay for unreacted $–NH_2$ / –NH– groups.[23]

Unlike C_3N_4 derived from melamine, amines are not a natural substituent for carbon phosphonitride. However, the peak observed at 2400 cm^{-1} is particularly unusual and therefore helps assessment tremendously. The first instinct is to assign this vibrational mode to nitriles in a chemically distinct environment from the species at 2200 cm^{-1}. However, an extensive survey of literature shows that in no compounds – whether organic, inorganic, or organometallic – are the C≡N stretching modes shifted to such a high frequency. The only fundamental vibrational modes that occur near 2400 cm^{-1} are the N-D / O-D stretch, P-H stretch, and S-H stretch.[24] Of these candidates, only P-H is a plausible functional group for our films.

Ultimately, the 2400 cm^{-1} mode (P-H), 3600 cm^{-1} – 2500 cm^{-1} mode (O-H), elevated oxygen content, and diminished nitrogen content can all be explained by partial hydrolysis of the films (**Figure 14**). At least some nitriles (C≡N) remain unreacted, as is evident in both IR (peak at 2200 cm^{-1}) and N1s XPS (~399 eV) spectra. Like $P(CN)_3$, it follows that, in the presence of atmospheric (or other sources of) moisture, these bonds hydrolyze to P-OH + HCN. In the case of C_3N_3P powder, such hydrolysis is probably limited to the surface[8], while CPN films appear to be sensitive throughout their thickness. P-OH accounts for the broad IR absorbance from 3600 cm^{-1} – 2500 cm^{-1} and contributes to the O1s XPS peak at ~533 eV.

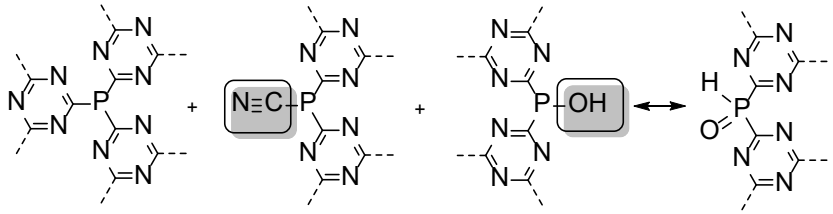

Figure 14. Illustration of likely chemical motifs in CPN films: phophorus-bridged triazines, unreacted nitriles, hydrolyzed phosphonous acids (P^{III}), and phosphine oxides (the P^{V} tautomer).

The P-H stretching mode observed at 2400 cm^{-1} is accounted for by tautomerization of P-OH to P(=O)H, illustrated schematically in **Figure 14**. Although unusual at first glance, this behavior is well documented for phosphinous and hypophosphinous (P^{III}) acids.[25-27] Hypophosphorous acid (H_3PO_2) exhibits strong bands at 2380 cm^{-1} for P-H stretching and 1180 cm^{-1} for P=O stretching[25],

while substituted compounds such as diphenyl phosphite show both O-H stretching at ~3500 cm^{-1} and P-H stretching at ~2300 cm^{-1} in solution[27].

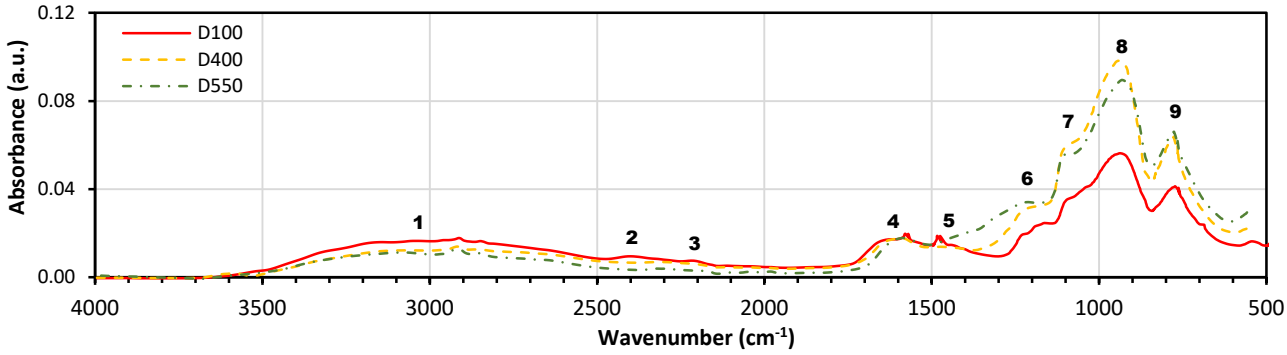

Figure 15. ATR-IR spectra of Batch D CPN samples with peaks labeled according to assignments from Table 2. Molecular diphenyl ether disappears at or below 400 °C. At 550 °C, P=O stretching shifts to higher wavenumber, indicating dehydration.

Substantial hydrolysis of P-CN bonds (~50–60%) can easily account for the increase in oxygen content and reduction in nitrogen content of solvothermally grown CPN films. Additionally, inclusions of diphenyl ether may account for the apparently high carbon content, offsetting the carbon lost to P-CN hydrolysis. The mechanism by which water was introduced to the CPN films is still a mystery, but XPS and IR spectra show that the chemistry of films produced by solvothermal growth (CPN) and thermally polymerized powders (C_3N_3P)[8] are qualitatively similar. Unfortunately, XPS proved only marginally useful for chemical analysis, as peak positions in literature are too variable to be positively assigned to single species in the CPN films.

Infrared spectra of CPN films heat treated above 100 °C change in small, but noticeable ways (**Figure 15**). The simplest is disappearance of the sharp vibrational modes associated with diphenyl ether (**Figure 15**, peaks 4 & 5). The weak intensity of the Ph_2O modes and breadth / overlap of peaks attributable to amorphous CPN precludes determination of whether molecular Ph_2O has evaporated at elevated temperature or if it otherwise decomposed and incorporated itself into the film. EDS (**Table 3**, D100–D550) shows negligible change in carbon and oxygen content versus temperature, suggesting Ph_2O pyrolysis rather than evaporation.

When analyzing changes in the broad peaks associated with amorphous CPN, it is important to note that the IR baseline changes substantially versus heat treatment temperature from 600 cm^{-1} – 1300 cm^{-1}. The shifting baseline is likely due to differences in film thickness, and therefore contributions from Si-O vibrational modes, as changes do not directly correlate with treatment temperature. With this in mind, there are two noteworthy chemical changes evident in IR spectra of the film. Firstly, the weak P-H (2400 cm^{-1}) and C≡N (2200 cm^{-1}) modes visible in sample D100 are absent in D400 and D550. For C≡N, this indicates completion of reaction of the dangling nitrile groups. A decrease in P-H intensity – which tracks with the decreasing P2p shoulder observed in XPS at 130.4 eV (**Figure 12**) – might result from a shift of the favored oxy phosphine tautomer from P(=O)H (hydride) to P-OH (hydroxyl), except the O-H stretching mode also weakens with increasing treatment temperature. Combined with a concurrent increase in intensity of the P=O

stretching vibrations, what likely occurs is dehydration of P-OH to P-O-P, shifting the tautomeric equilibrium away from hydride form to hydroxyl form. Substantial bimolecular dehydration of phosphoric acid to pyrophosphate ($H_4P_2O_7$) is observed at 170 °C, consistent with our observations.[28]

Secondly, when heating to the highest temperature, 550 °C, the asymmetric P=O stretching mode initially observed at 1190 cm^{-1} appears to shift and broaden toward 1400 cm^{-1}. This behavior is indicative of multiple dehydration, forming clusters with phosphorus pentoxide–like structure (T2-symmetric P=O stretch ≈ 1400 cm^{-1} in P_4O_{10}).[29] Unlike bimolecular dehydration, which may proceed between adjacent phosphines at lower temperatures, the polymolecular processes necessary for 3- and 4-center crosslink formation are only likely at temperatures high enough for the less common bis-hydroxyl substituted phosphines to encounter each other.

Chemical and morphological analyses showed that CPN films with similar chemistry to bulk C_3N_3P can be grown from $P(CN)_3$ solution. Although hydrolysis of unreacted nitriles is clearly a concern, films are stable to at least 550 °C, according to IR spectroscopy. Since the original goal was to make elastic materials with good thermooxidative stability, the next step was to perform mechanical analyses on these films to determine their viscoelastic behavior.

Mechanical Analysis

CPN films were 1–2 μm after 7 days of deposition, and despite some amount of adhered particulate, they were uniform enough to perform mechanical analysis of hardness (H) and reduced elastic modulus (E_r) by nanoindentation. Nanoindentation was performed on films heated to 100, 250, 400, and 550 °C under dynamic vacuum for 4 hours to assess the mechanical properties (e.g., reduced modulus, hardness) thereof. Although reduced modulus is related to Young's modulus by Poisson's ratio, ν, (when), Poisson's ratio for our CPN films is unknown, thus only is reported herein for the samples measured. For the majority of materials, however, 0 (cork) > ν ≥ 0.5 (rubber), meaning that the value of Young's modulus is expected to be 75% – 100% of the reduced modulus as reported.[30] To ensure that the measured hardness and modulus represented those of the films and not the quartz substrates, only indents with a contact depth below 10% of the coating thickness are reported for Batches A and D (**Figure 11**). Nanoindentation was also carried out on Batches B and C, with comparable results, but as the film thickness was not measured, the results should be considered semi-quantitative and are not reported herein. The cutoff of 100 nm is justified given the roughly 1 μm length scale of film thickness.[31] The reported values represent the average and standard deviation of at least nine indents.

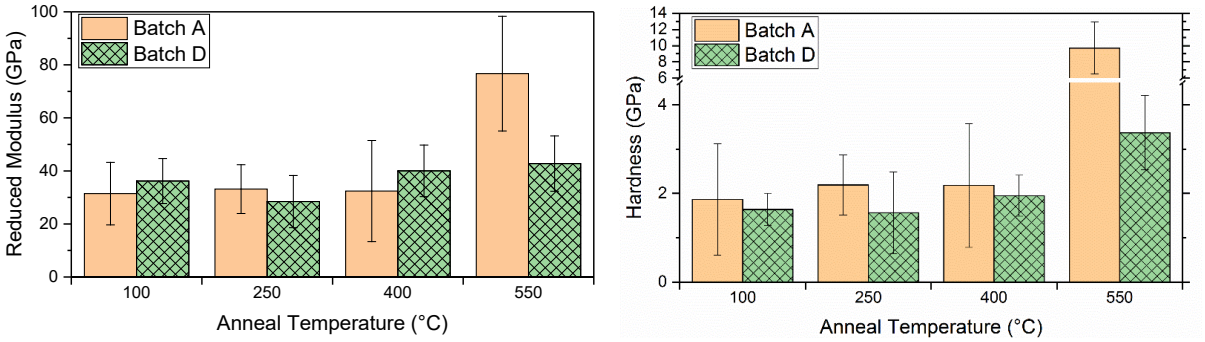

Figure 16. Calculated reduced elastic moduli and hardness (in compression) of heat treated samples from Batches A and D. Means and standard deviations from multiple indentations are represented by bar heights and error bars, respectively.

The reduced modulus for the films treated at 100, 250, and 400° C fell between 20 and 40 GPa on average (**Figure 16**). For the 550° C anneal temperature, the average reduced modulus of Batch A was roughly 80 GPa while Batch D was roughly 40 GPa. Hardness followed a similar trend; films treated at 100 – 400° C fell between 1.5 and 2 GPa for both batches. The average hardness of the 550° C anneal temperature was roughly 9 GPa for Batch A and roughly 4 GPa for Batch D. No adhesive forces were measured between the sample and indenter for any heat treatment temperature. Surprisingly little variability in the average values of and H was observed for heat treatment temperatures between 100 °C and 400 °C, indicating minimal structural evolution of films under these conditions (either chemical or morphological). As they are heated to 550 °C, films clearly do evolve, although the variability in both (±15 GPa) and H (±2.6 GPa) from batch to batch is substantial.

Initially, it was suspected that the increase in apparent modulus and hardness on annealing at 550 °C might be attributable to crystallization of the film, a change in thickness (thus increasing substrate effects on indentation), or a change in elemental composition. However, grazing incidence XRD showed no crystallization, and elemental composition was shown to be unchanged (to within error) by both XPS and EDS (**Table 3**). Thickness is unlikely to be the cause, either, as the only data included in statistical analyses were those where contact depths calculated by the Oliver and Pharr method[19] were <10% of film thickness measured by SEM. A plausible explanation for increased hardness and modulus after heat treatment at 550 °C is increased crosslink density due to multi-center P-OH dehydration. Two-center dehydration reactions that occur between adjacent phosphines should minimally affect mechanical properties; these moieties are already close together on the carbon phosphonitride backbone. Multi-center P-O clusters, however, require P-$(OH)_2$ groups which more sparsely populate the CPN backbone, chemically linking parts of the backbone which would otherwise deform independently.

For films annealed at or below 400 °C, the reduced modulus and hardness are = 26.5 ± 1.5 GPa and = 1.5 ± 0.1 GPa, respectively (average ± standard error). The modulus and hardness of solvothermally grown CPN are about an order of magnitude lower than amorphous diamond-like carbon (DLC), in the ranges of = 60–210 GPa and = 12–30 GPa, respectively.[32] Sputtered carbon nitride films (CN_x where $x \leq 0.5$), common tribological coatings, are similarly about an order of

magnitude higher than those measured in the present study, where = 105–260 GPa and = 7–28 GPa.[33]

Notably, CPN films compare favorably to high performance polymers like Kevlar, measured to have reduced modulus and hardness of = 20.3 ± 1.6 GPa and = 1.3 ± 0.7 GPa *via* nanoindentation, respectively.[34] Additionally, falls in line with graphitic carbon nitride (*g*-C_3N_4) prepared by high temperature pyrolysis and vacuum sublimation (= 30 GPa)[23]. Hardness only approaches *g*-C_3N_4 (= 6.2 GPa)[23] on annealing to 550 °C (= 5.0 ± 0.4 GPa), at which atomic mobility promotes the formation of multi-center crosslinks by P-OH dehydration. A reduction in microporosity at the highest heat treatment temperatures is also plausible – and would have a significant effect on hardness[35,36] – but was not independently investigated by attempted measurement of film density.

Although these results show that P(CN)3 can be processed into monolithic films, the properties of the films are those of a hard coating, not a viscoelastic material. Additionally, growth of these films is slow (1–2 μm per week), so applications are limited to comparatively thin films.

Synthesizing Novel Cyanophosphine Monomers

Since it was found that $P(CN)_3$ produces thermoset materials that are hard and brittle due to their high crosslink density, methods for modifying the chemistry of cyanophosphines to produce more favorable (i.e. elastomeric) materials were sought. Reducing the number of cyano (-C≡N) groups on each phosphorus should result in materials with lower crosslink density but similar overall polymerization chemistry. Some dicyano- and monocyano-phosphines have been reported in literature, but like $P(CN)_3$, they had not been investigated as monomers.[12] Additionally, the traditional method of synthesizing cyanophosphines using AgCN is rather cost-prohibitive, and alternative cyanating reagents (e.g. TMS-CN[37-42], LiCN[43,44]) that have been investigated are not much less expensive.

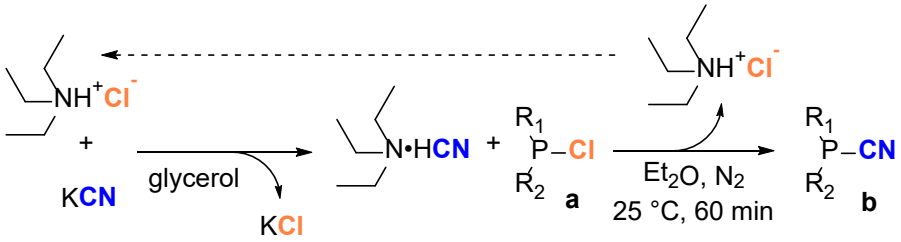

Figure 2. Reaction schematic for the use of triethylammonium chloride, KCN, and chlorophosphine to synthesize the correspond cyanophosphine. Chlorine (orange) and cyanide (blue) are highlighted to facilitate tracking the exchange of active species across steps.

Based on prior literature, the scheme illustrated in **Figure 2** (copied above for convenience) was devised to synthesize a broad range of monocyano- and dicyano-phosphine monomers bearing organic substituents on the remainder of free phosphorus sites. Compared to using AgCN, LiCN, or TMS-CN these reactions require relatively inexpensive reagents and solvents, in addition to chlorophosphines, a wide range of which are commercially available. A series of monochloro- and

dichloro-phosphines bearing variant organic substituents (e.g., aliphatic and aromatic hydrocarbons, amines) were tested for reactivity toward HCN generated *in situ* by this methodology. The results of successful syntheses using these chlorophosphines – detailed in **Methods: Synthesis** – are summarized in **Table 5**, below.

Table 5. Isolated yields† of cyanophosphine products after reacting corresponding chlorides with alkylammonium cyanide

2 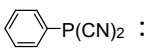 : 66%	**3** 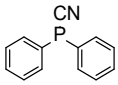 : 96%
4 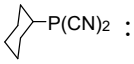 : 90%	**5** 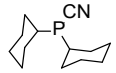 : 73%
6 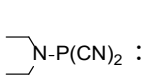 : 73%	**7** 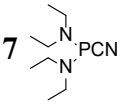 : 82%

† After filtration, evaporation of solvent, and distillation of product

Compounds **2-7** have all been previously reported in literature[12], but the relatively high yields in which they were isolated using this method show that it is broadly applicable to a variety of cyanophosphine products. The general protocol that was settled upon was adding a 2 M solution of substrate in Et_2O to 1.1 equivalents of 1 M triethylammonium cyanide adduct in Et_2O (TEACN) at 25 °C under N_2, followed by 30–60 min of stirring, filtration of solids, concentration of the filtrate, and distillation of the product therein. Identification of appropriate conditions for both the preparation of TEACN and its subsequent reaction with chlorophosphines required testing various solvents and conditions for each reaction.

In situ preparation of HCN was identified early on as being an important component of this synthesis, as it is a volatile (BP_{HCN} = 26 °C), toxic liquid that is not easily acquired from commercial vendors due to issues with potential runaway (exothermic) polymerization during transport.[45] Such physical and health hazards are significantly mitigated by generating it on site, complexing it with an amine (decreasing its volatility), keeping it cool, and consuming it directly after generation with minimal handling. To this end, it was found that reacting potassium cyanide with triethylamine hydrochloride (TEACl) was an efficient way to simultaneously generate HCN and a tertiary amine *in situ*. Both are volatile and can be distilled, driving the equilibrium toward products. This reaction requires a highly polar, nonvolatile solvent to both solubilize the salts and prevent distillation of the solvent. Although dimethylethylene diamine (BP_{DMEDA} = 120 °C), ethylene glycol (BP_{EG} = 197 °C), and sulfolane (1,4-tetramethylene sulfone, $BP_{sulfolane}$ = 285 °C) were all investigated as potential solvents, the former distilled at 100 °C, whereas sulfolane was insufficiently polar to dissolve starting materials. It was eventually found that glycerol ($BP_{glycerol}$ = 290 °C) was polar enough to dissolve both reagents and sufficiently non-volatile to remain entirely in the distillation flask. Additionally, vacuum distillation of glycerol (~150 °C) prior to use is sufficient to remove dissolved water; water was not observed in the distillate of reactions using vacuum distilled glycerol to generate HCN, nor was hydrolysis observed in the

cyanophosphine products. The distillation apparatus used for the preparation of TEACN is illustrated in **Figure 17**, below.

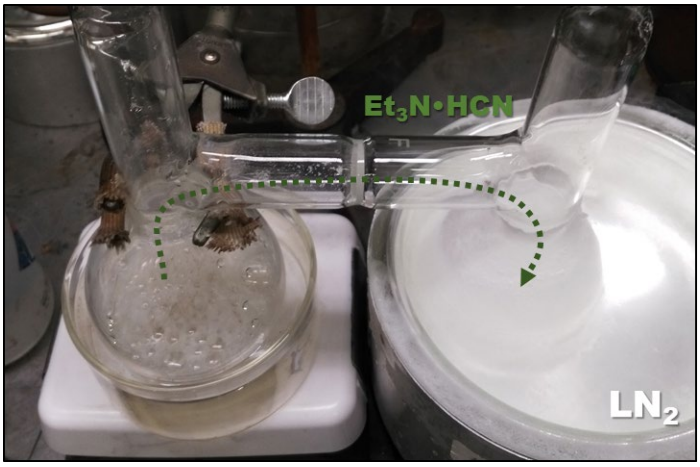

Figure 17. Distillation setup for preparing TEACN (the liquid adduct of triethylamine and hydrogen cyanide) *in situ* by reacting KCN with triethylamine hydrochloride (TEACl) in glycerol. TEACN can be isolated or used as-collected in subsequent reactions.

Most of the cyanophosphine products isolated were colorless oils at room temperature (or exhibited low melting points). Low melting points are desirable for achieving monolithic, glassy or elastomeric solids by thermosetting these neat cyanophosphines. However, the relatively small steric bulk of the organic groups on these cyanophosphines, while making them amenable to vacuum distillation for purification, also makes them prone to the same volatility issues observed in $P(CN)_3$ at temperatures sufficiently high for thermosetting (200+ °C). To overcome issues with volatility, a new cyanophosphine monomer – bis(diphenylamino)cyanophosphine ($(Ph_2N)_2PCN$), **8a** – was synthesized in a one-pot, two step reaction, illustrated in **Figure 3** (copied below for convenience).

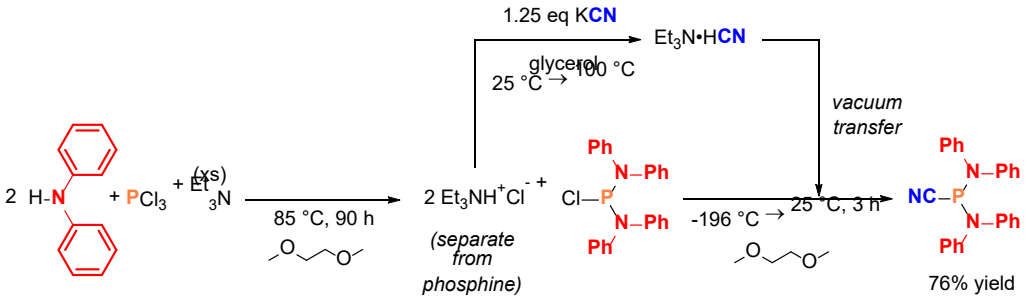

Figure 3. The synthesis of aminocyanophosphines from PCl_3, diphenylamine, and KCN by incorporating the procedure illustrated in **Figure 2**. Key components of the final product are highlighted in red (Ph_2N), orange (P), and blue (CN).

Diphenylamine turns out to be a substituent that is advantageous for several reasons. Firstly, the aromatic phenyl groups should be relatively thermally stable and provide enough bulk that the corresponding cyanophosphine (MW = 393.41 g mol^{-1}) is essentially non-volatile. Secondly, the steric bulk of the diphenylamino group means that reaction with PCl_3 does not give a statistical

mixture of mono-, di-, and tri-substituted products, but instead gives either ***solely*** mono-substituted or di-substituted product depending upon the temperature at which the reaction is run. Conveniently, the hydrochloric acid formed from the reaction to make the chlorophosphine is easily removed by reaction with triethylamine, which in turn is consumed during the second part of the reaction generating HCN. All that is required between the first and second parts of the reaction is a filtration step (facilitated by using an H-tube with a fritted glass filter) separating TEACl and chlorophosphine intermediate. While this intermediate ($(Ph_2N)_2PCl$) can be separated and purified before the subsequent step, its purification is unnecessary. The structure of the novel cyanophosphine monomer, bis(diphenylamino)cyanophosphine, was confirmed by both NMR spectroscopy and single crystal x-ray diffraction.

Liquid Cyanophosphine Thermosets

While compounds **2-7** were all qualitatively found to thermoset (heating in sealed scintillation vials on a hot plate), only the most promising, phenyldicyanophosphine ($PhP(CN)_2$, **2a**), was selected for further testing. This compound has the most stable organic substitutent (a phenyl group) of compounds **2-7** while exhibiting a relatively low vapor pressure, low melting point, and good reactivity toward thermosetting. Since 2a is sufficiently volatile to be vacuum distillable, thermosetting was performed in a quartz crucible sealed within a Teflon cup in a Parr acid digestion bomb at 250 °C, as described in **Methods: Synthesis**. The isolated product, **2b**, is shown in **Figure 18**, below.

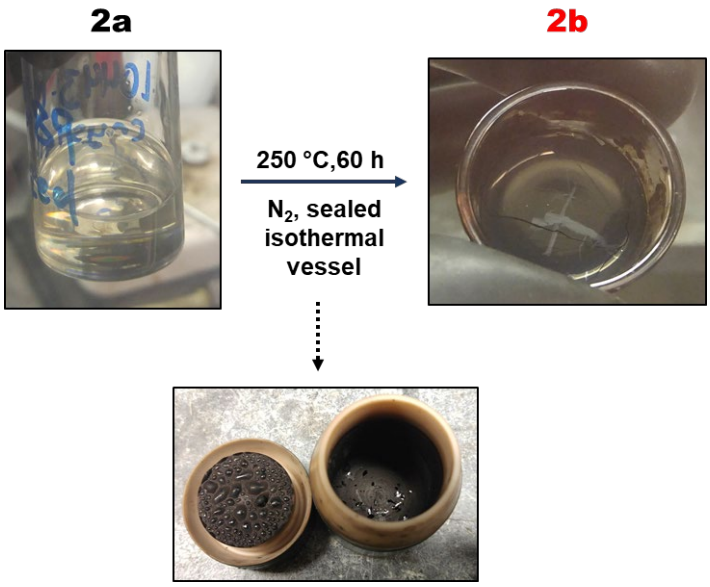

Figure 18. Starting material (**2a**, left) and product (**2b**, right) from the thermosetting of $PhP(CN)_2$ at 250 °C in a Parr acid digestion bomb.

As can be seen in **Figure 18**, **2b** is a hard thermoset, rather than a thermoplastic / elastomer. This is perhaps not surprising, since the monomer bears two –C≡N groups that can each react with two –C≡N groups on other monomers, leading to a highly crosslinked product. It was found via thermogravimetric analysis that the thermooxidative stability of **2b** is quite good (**Figure 19**).

Despite the organic phenyl group, decomposition of **2b** in air only proceeds to a meaningful extent above 500 °C. While not as good as the thermooxidative stability of C_3N_3P (thermoset $P(CN)_3$), thermoset $PhP(CN)_2$ exhibits excellent air stability for a material where 60% of its mass is carbon and 18% is nitrogen.

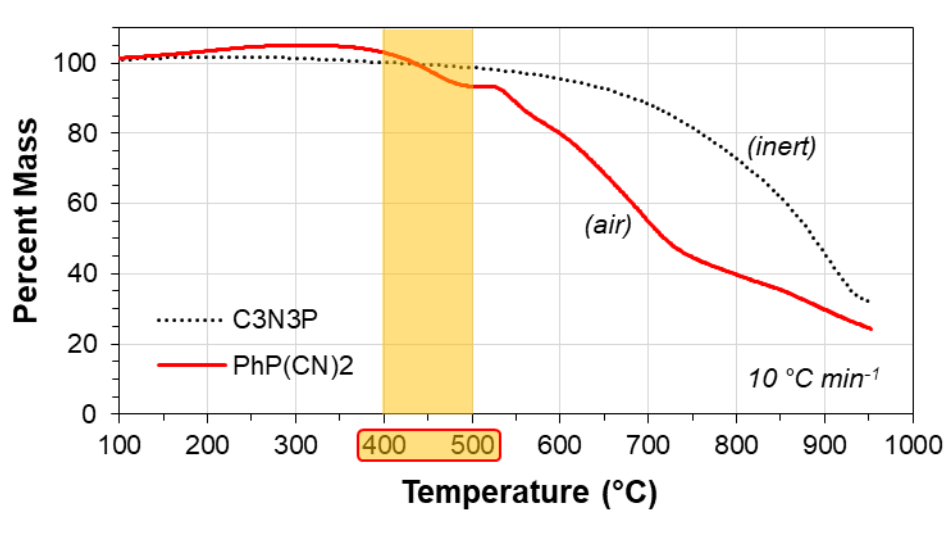

Figure 19. Thermogravimetric analyses (TGA) of **2b** under air (solid line) and thermoset $P(CN)_3$ (dotted line), for reference.

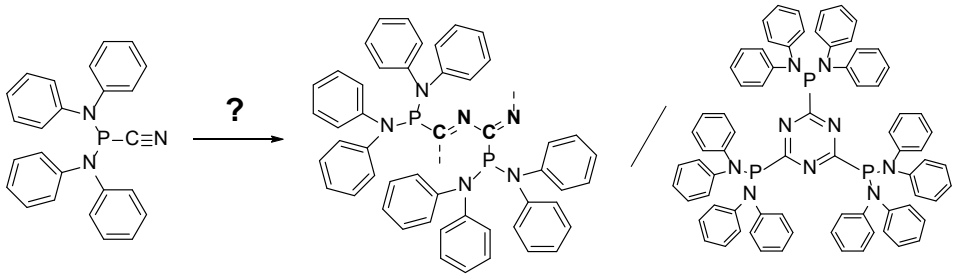

Figure 20. Hypothetical thermosetting reactions of bis(diphenylamino)cyanophosphine, **8a**.

Compound **8a**, bis(diphenylamino)cyanophosphine, was synthesized in response to the results obtained from the thermosetting of **2a**. Diphenylamino groups were selected for the organic substituents because they provide a great deal of mass (reducing volatility of the monomer), should exhibit decent thermal stability, and can be precisely mono- or di-substituted on phosphorus as a result of their steric bulk. From the results of the thermosetting of **2a**, it was already known that monomers with two cyano substituents will not produce thermoplastic. While it was possible, per **Figure 20**, **8a** would only trimerize on heating, the possibility also existed that linear –C=N– polymers could be formed, resulting in a thermoplastic product. Whether 8a could be thermally polymerized into a thermoplastic material was tested by heating ~1 gram of 8a in a sealed Pyrex tube, as described in **Methods: Synthesis** and illustrated in **Figure 21**, below.

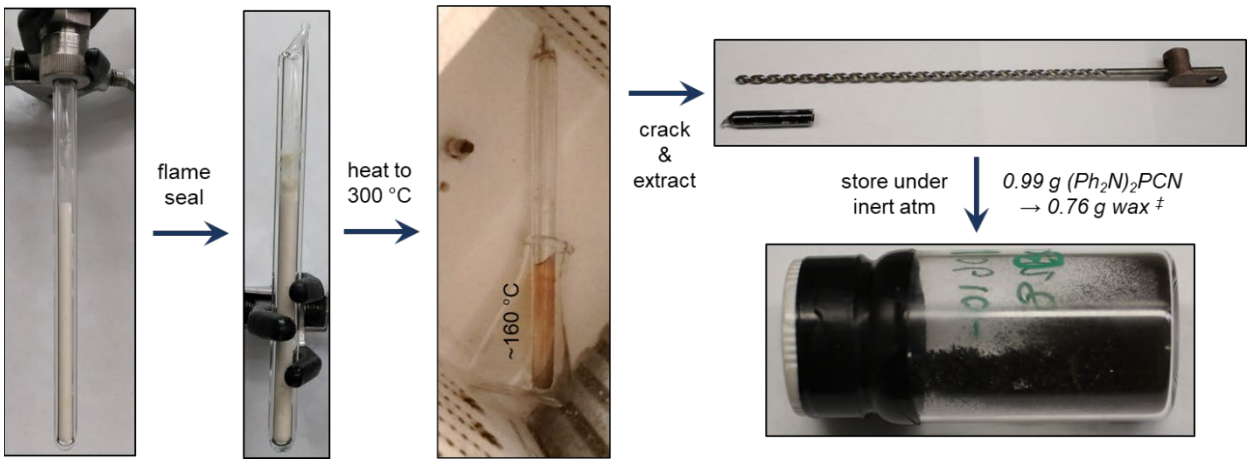

Figure 21. Thermosetting **8a** ($(Ph_2N)_2PCN$) in a sealed Pyrex tube, slowly heating from room temperature to 350 °C. The product, **8b**, is isolated as a waxy, black solid.

After heating to 350 °C overnight, the resulting product (**8b**) was found to be a waxy, black solid capable of re-melting at ~150 °C. These results were extremely promising, so TGA was subsequently performed to assess the thermal stability of **8b** (**Figure 22**). Surprisingly, **8b** is thermally unstable even under inert atmosphere, quite unlike thermoset $P(CN)_3$ and $PhP(CN)_2$. Mass lost is observed at as low as 170 °C, with gradual loss of up to 55% the initial mass of sample above 600 °C, leaving behind a shiny, brittle chunk of solid in the alumina TGA pan. To investigate the origin of this mass loss, DSC was subsequently performed to analyze any decomposition reactions that might be occurring (**Figure 23**). Curiously, not only was no major endo- or exotherm observed up to 300 °C (well above the temperature at which mass lost began in TGA), but there was a large, sharp melting point observed at ~45 °C.

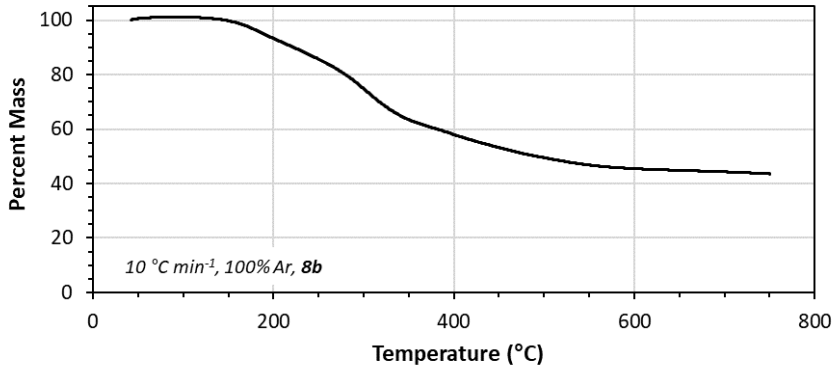

Figure 22. Thermogravimetric analysis of **8b** under flowing Ar, showing low thermal stability. Approximately 55% of the initial mass is lost by 600 °C, leaving behind a brittle, graphitic chunk.

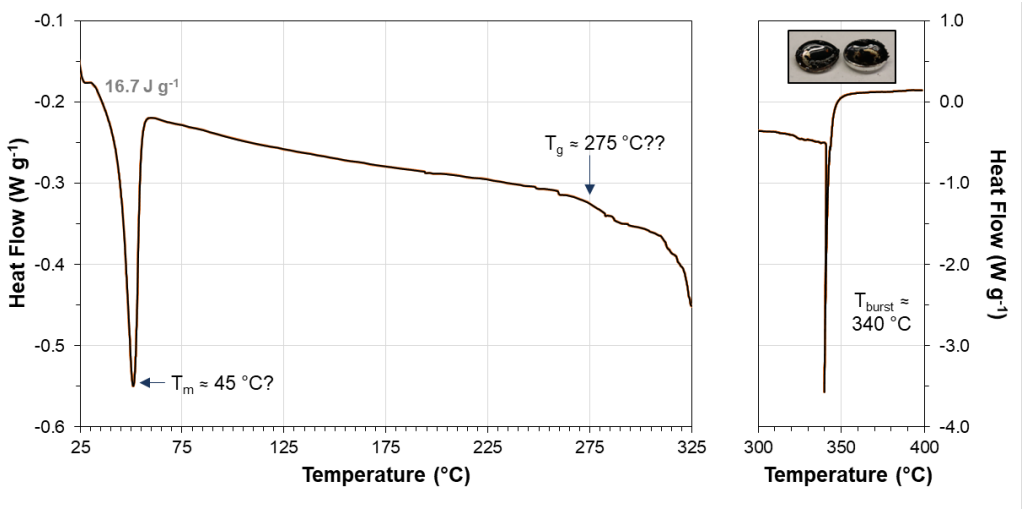

Figure 23. Differential scanning calorimetry of **8b** in a sealed pan, showing a distinct melting point at ~45 °C (Ph_2NH), an apparent glass transition at ~275 °C, and rupture pan at ~340 °C.

On further investigation under a microscope, it was found that embedded within the black, glassy wax were a plethora of large, crystalline solids, shown in **Figure 24**. This secondary phase was analyzed by Raman spectroscopy and NMR in $CDCl_3$ (which dissolves the crystallites, but not the bulk of the wax). Combining results from Raman, NMR, and the melting point observed in DSC, it is apparent that this secondary phase is diphenylamine (Ph_2NH), which is especially surprising considering that there are no labile protons in **8a**. For this secondary phase to form (volatilization of which is likely the cause of mass loss at low temperatures in TGA), diphenylamine substituents on phosphorus must be stripping protons from aromatic groups in the structure.

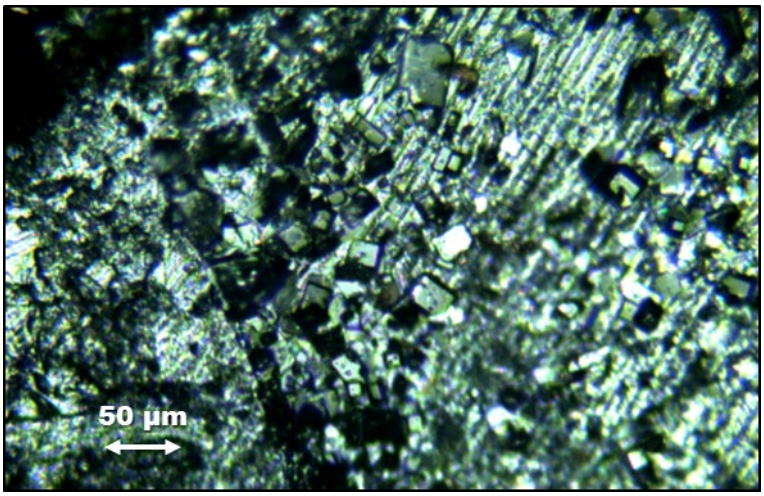

Figure 24. Optical image of **8b** wax taken in a confocal Raman microscope, showing large crystalline chunks (Ph_2NH) within the glassy matrix.

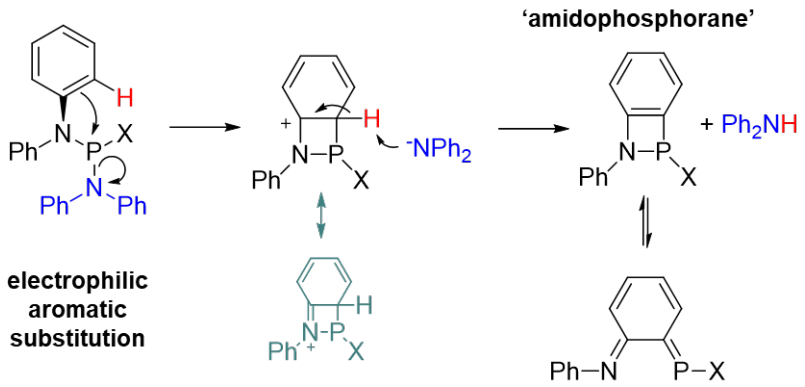

Figure 25. Proposed mechanism for the non-oxidative degradation of **8b** by intramolecular electrophilic aromatic substitution and subsequent elimination of diphenylamine (Ph_2NH).

It is hypothesized that the non-oxidative decomposition of **8b** occurs by a mechanism similar to the one illustrated in **Figure 25**, which can account for the formation of Ph_2NH despite the monomer and polymer lacking labile protons. Although such an intramolecular electrophilic aromatic substitution forming a vicinal imidophosphorane looks extremely unusual, there are examples of such structures in literature.[46] The strained four-membered N-P ring is in fact stabilized by resonance with a less strained structure of four conjugated double bonds. As to the reason why such a reaction appears facile in 8b, the likely explanation is that not only do cyano substituents on phosphorus increase its electrophilicity ($P(CN)_3$ is a potent electron acceptor), but the adjacent aromatic amine also stabilizes the carbocation formed by such a reaction through resonance and donation of electron density from its lone pair.

Unfortunately, the structure of **8b** is uniquely unstable due to the combination of proximal cyanophosphine and aromatic amine. It is likely that this undesired intramolecular decomposition reaction could be stopped by removing accessible phenyl protons or by increasing steric bulk to hinder formation of the strained four-membered imidophosphorane intermediate. Such changes to the structure provide a path forward for these materials as thermally stable thermoplastics, but require significant further study.

REFERENCES

(1) Chaloux, B.L.; Shockley, J.M.; Wahl, K.J.; Tsoi, S.; Birnbaum, A.J.; Epshteyn, A. "Mild Solvothermal Growth of Robust Carbon Phosphonitride Films." *Chem. Mater.* **2018**, *30*, 6082-6090.

(2) Chaloux, B.L.; Fu, E.; Maza, W.A.; Epshteyn, A. "Triethylammonium cyanide: A recyclable reagent for cyanophosphine synthesis." *254th ACS National Meeting* Washington, D.C., 2017.

(3) Fergus, J.W. "Sealants for solid oxide fuel cells." *J. Power Sources* **2005**, *147*, 46-57.

(4) Rhein, R.A. *Thermally Stable Elastomers: A Review*, Naval Weapons Center, China Lake, 1983.

(5) Camino, G.; Lomakin, S.M.; Lazzari, M. "Polydimethylsiloxane thermal degradation Part 1. Kinetic aspects." *Polymer* **2001**, *42*, 2395-2402.

(6) Sugama, T.; Pyatina, T.; Redline, E.; McElhanon, J.; Blankenship, D. "Degradation of different elastomeric polymers in simulated geothermal environments at 300 °C." *Polym. Degrad. Stab.* **2015**, *120*, 328-339.
(7) Sugama, T.; Pyatina, T.; Redline, E.; McElhanon, J.; Blankenship, D. *Evaluation of the Performance of O-rings Made with Different Elastomeric Polymers in Simulated Geothermal Environments at 300°C*, U.S. Department of Energy, Energy Efficiency and Renewable Energy Program, 2014.
(8) Chaloux, B.L.; Yonke, B.L.; Purdy, A.P.; Yesinowski, J.P.; Glaser, E.R.; Epshteyn, A. "$P(CN)_3$ Precursor for Carbon Phosphonitride Extended Solids." *Chem. Mater.* **2015**, *27*, 4507-4510.
(9) Lange, J.; Luisier, A.; Hult, A. "Influence of crosslink density, glass transition temperature and addition of pigment and wax on the scratch resistance of an epoxy coating." *Journal of Coatings Technology* **1997**, *69*, 77-+.
(10) Ahmed, S.; Nakajima, T.; Kurokawa, T.; Haque, M.A.; Gong, J.P. "Brittle-ductile transition of double network hydrogels: Mechanical balance of two networks as the key factor." *Polymer* **2014**, *55*, 914-923.
(11) Wang, Q.; Strobel, T.A. Geophysical Laboratory, Carnegie Institution of Washington, Washington, D.C. Personal communication, September 8, 2016.
(12) Coskran, K.J.; Jones, C.E. "Synthesis and spectroscopic properties of some cyanophosphines." *Inorg. Chem.* **1971**, *10*, 1536-1537.
(13) Nöth, H.; Vetter, H.-J. "Dialkylamino-phosphane, II. Darstellung und Reaktionen von Dimethylamino-halogen-phosphanen, $(Me_2N)_{3-n}PX_n$[3])." *Chem. Ber.* **1963**, *96*, 1109-1118.
(14) Petrov, K.A.; Gatsenko, L.G.; Neimysheva, A.A. "EFIRY ALKILTSIANFOSFINOVYKH KISLOT." *Zh. Obshch. Khim.* **1959**, *29*, 1827-1831.
(15) Johns, I.B. "CN Compounds". U.S. Patent 3,410,809, Nov 12, 1968.
(16) Schwesinger, R.; Willaredt, J.; Schlemper, H.; Keller, M.; Schmitt, D.; Fritz, H. "Novel, Very Strong, Uncharged Auxiliary Bases - Design and Synthesis of Monomeric and Polymer-Bound Triaminoiminophosphorane Bases of Broadly Varied Steric Demand." *Chem. Ber. Recl.* **1994**, *127*, 2435-2454.
(17) Link, R.; Schwesinger, R. "A Safe Synthesis of Diphosphazenium Salts." *Angewandte Chemie-International Edition in English* **1992**, *31*, 850-850.
(18) Davies, R.H.; Finch, A.; Gardner, P.J.; Hameed, A.; Stephens, M. "Standard Enthalpies of Hydrolysis and Formation of Tricyanophosphine." *J. Chem. Soc., Dalton Trans.* **1976**, 556-558.
(19) Oliver, W.C.; Pharr, G.M. "An Improved Technique for Determining Hardness and Elastic-Modulus Using Load and Displacement Sensing Indentation Experiments." *J. Mater. Res.* **1992**, *7*, 1564-1583.
(20) Xie, X.; Fan, X.; Huang, X.; Wang, T.; He, J. "In situ growth of graphitic carbon nitride films on transparent conducting substrates via a solvothermal route for photoelectrochemical performance." *RSC Adv.* **2016**, *6*, 9916-9922.
(21) Volkert, C.A.; Minor, A.M. "Focused ion beam microscopy and micromachining." *MRS Bull.* **2007**, *32*, 389-395.
(22) Averett, L.A.; Griffiths, P.R.; Hishikida, K. "Effective path length in attenuated total reflection spectroscopy." *Anal. Chem.* **2008**, *80*, 3045-3049.
(23) Purdy, A.P.; Callahan, J.H. "Syntheses of Sublimable Carbon Nitride Materials." *Main Group Chem.* **1998**, *2*, 207-213.

(24) Socrates, G. *Infrared and Raman characteristic group frequencies : tables and charts*; 3rd ed.; Wiley: Chichester ; New York, 2001.
(25) Lovejoy, R.W.; Wagner, E.L. "Infrared Spectra of Hypophosphorous Acid + Its Salts." *J. Phys. Chem.* **1964**, *68*, 544-550.
(26) Pietro, W.J.; Hehre, W.J. "Tautomerization of Dimethyl Phosphonate." *J. Am. Chem. Soc.* **1982**, *104*, 3594-3595.
(27) Christiansen, A.; Li, C.Z.; Garland, M.; Selent, D.; Ludwig, R.; Spannenberg, A.; Baumann, W.; Franke, R.; Borner, A. "On the Tautomerism of Secondary Phosphane Oxides." *Eur. J. Org. Chem.* **2010**, 2733-2741.
(28) Higgins, C.E.; Baldwin, W.H. "Dehydration of Orthophosphoric Acid." *Anal. Chem.* **1955**, *27*, 1780-1783.
(29) Jensen, J.O.; Banerjee, A.; Zeroka, D.; Merrow, C.N.; Gilliam, S.J.; Kirkby, S.J. "A theoretical study of P4O10: vibrational analysis, infrared and Raman spectra." *Spectrochim. Acta, Part A* **2004**, *60*, 1947-1955.
(30) Greaves, G.N.; Greer, A.L.; Lakes, R.S.; Rouxel, T. "Poisson's ratio and modern materials." *Nat. Mater.* **2011**, *10*, 823-837.
(31) Saha, R.; Nix, W.D. "Effects of the substrate on the determination of thin film mechanical properties by nanoindentation." *Acta Mater.* **2002**, *50*, 23-38.
(32) Savvides, N.; Bell, T.J. "Microhardness and Young Modulus of Diamond and Diamond-Like Carbon-Films." *J. Appl. Phys.* **1992**, *72*, 2791-2796.
(33) Quiros, C.; Nunez, R.; Prieto, P.; Vergara, I.; Caceres, D.; Soriano, L.; Fuentes, G.G.; Elizalde, E.; Sanz, J.M. "Correlation between bonding structure and mechanical properties of amorphous carbon nitride thin films." *Surf. Coat. Technol.* **2000**, *125*, 284-288.
(34) Bencomo-Cisneros, J.A.; Tejeda-Ochoa, A.; Garcia-Estrada, J.A.; Herrera-Ramirez, C.A.; Hurtado-Macias, A.; Martinez-Sanchez, R.; Herrera-Ramirez, J.M. "Characterization of Kevlar-29 fibers by tensile tests and nanoindentation." *J. Alloys Compd.* **2012**, *536*, S456-S459.
(35) He, L.H.; Standard, O.C.; Huanga, T.T.Y.; Latella, B.A.; Swain, M.V. "Mechanical behaviour of porous hydroxyapatite." *Acta Biomater.* **2008**, *4*, 577-586.
(36) Luo, J.; Stevens, R. "Porosity-dependence of elastic moduli and hardness of 3Y-TZP ceramics." *Ceram. Int.* **1999**, *25*, 281-286.
(37) Lazukina, L.; Kukhar, V.; Romanov, G.; Khaskin, G.; Dubinina, T.; Ofitserov, E.; VOLKOV, V.; Pudovik, A. "Reactions of trimethylsilyl cyanide with phosphorus and sulfur acid chlorides." *ChemInform* **1980**, *11*.
(38) Horner, L.; Lindel, H. "Organo-Phosphorus Compounds .3. Phosphinic and Thiophosphinic Cyanides as Fluorescent Sh-Selective Reagents." *Chemische Berichte-Recueil* **1985**, *118*, 676-682.
(39) Romanov, G.V.; Semkina, É.P.; Pudovik, A.N. "Dibutyl cyanophosphite and its properties." *Bulletin of the Academy of Sciences of the USSR, Division of chemical science* **1989**, *38*, 630-631.
(40) Maraval, A.; Igau, A.; Lepetit, C.; Chrostowska, A.; Sotiropoulos, J.-M.; Pfister-Guillouzo, G.; Donnadieu, B.; Majoral, J.P. "Cyanophosphine Derivatives: Nitrile or Cyanide Functionality?" *Organometallics* **2001**, *20*, 25-34.
(41) Kingston, J.V.; Ellern, A.; Verkade, J.G. "A stable structurally characterized phosphorus-bound isocyanide and its thermal and catalyzed isomerization to the corresponding cyanide." *Angewandte Chemie-International Edition* **2005**, *44*, 4960-4963.

(42) Henne, F.D.; Dickschat, A.T.; Hennersdorf, F.; Feldmann, K.O.; Weigand, J.J. "Synthesis of Selected Cationic Pnictanes [LnPnX3–n]n+ (L = Imidazolium-2-yl; Pn = P, As; n = 1–3) and Replacement Reactions with Pseudohalogens." *Inorganic Chemistry* **2015**, *54*, 6849-6861.
(43) Rossmanith, K. "Neue Wege zur Herstellung von reinem Lithiumcyanid und Lithiumcyanoargentat." *Monatshefte für Chemie und verwandte Teile anderer Wissenschaften* **1965**, *96*, 1690-1694.
(44) Johns, I.B.; DiPietro, H.R. "Synthesis and Reactions of Anhydrous Lithium Cyanide1." *The Journal of Organic Chemistry* **1964**, *29*, 1970-1971.
(45) Gause, E.H.; Montgomery, P.D. "Hydrogen Cyanide Stability and Heat of Polymerization." *Journal of Chemical & Engineering Data* **2002**, *5*, 351-354.
(46) Hounjet, L.J.; Caputo, C.B.; Stephan, D.W. "Phosphorus as a Lewis Acid: CO2Sequestration with Amidophosphoranes." *Angew. Chem. Int. Ed.* **2012**, *51*, 4714-4717.